https://doi.org/10.1016/j.jpowsour.2020.228454

Carbon-free Sustainable Energy Technology: Direct Ammonia Fuel Cells

Yuqi Guo, Zhefei Pan, Liang An*

Department of Mechanical Engineering, The Hong Kong Polytechnic University, Hung Hom, Kowloon, Hong Kong SAR, China

* Corresponding author.

Email: liang.an@polyu.edu.hk (L. An)

Abstract:

The potential safety issues and expensive cost for hydrogen storage hinder the development of fuel cell vehicles and other power generation applications. Ammonia, an indirect hydrogen storage media containing a high content of hydrogen (17.8 wt. %), could be an ideal carbon-free fuel for fuel cells. As such, direct ammonia fuel cells (DAFCs) have attracted ever-increasing attention in the past years. The DAFCs employed alkaline anion exchange membranes (AEMs), referring to the low temperature AEM-DAFCs, not only have merits of the high energy efficiency, but are compatible with non-precious catalysts without ammonia decomposition process, which means a lower cost compared to proton exchange membrane fuel cells. Unlike high-performance of direct ammonia solid oxide fuel cells (high temperature SO-DAFCs), the low catalytic activity of the electro-catalysts and the difficulty of ammonia oxidation at low temperatures lead to far worse performance of low temperature AEM-DAFCs. Therefore, this article is trying to offer some incentives and indicate a direction for the future development of DAFCs. First, this review emphasizes previous development tracks and current progress on low temperature AEM-DAFCs and high temperature SO-DAFCs. For the low temperature AEM-DAFCs, the current progress of platinum-based and non-platinum-based electro-catalysts, high conductivity membranes, the low catalytic activity and membrane degradation issues will be summarized. The

performance comparison of high temperature SO-DAFCs with various electrode and electrolyte materials and NO_x formation issues will be discussed in the later section.

Keywords: Ammonia oxidation reaction; direct ammonia fuel cells; anion exchange membrane; solid oxide; electro-catalysts

1. Introduction

The extensive use of fossil fuels in various areas, such as industrial and transportation, etc. have arisen some issues for the environment and human health. Around 0.4 per cent of carbon oxide concentration annually pile up in the atmosphere, resulting from the massive consumption of fossil fuels and deforestation [1], which may lead to climate change, rises in sea level and frequency of extreme weather events. In order to alleviate those adverse effects of using fossil fuels, hydrogen, an alternative sustainable source, was applied to achieve the zero-carbon emission target. Although the renewable electricity produced from the solar, wind energy system drives the water splitting process to form the green hydrogen, the cost-effective hydrogen storage remains a tricky part for the hydrogen economy, due to the low volumetric density of hydrogen gas [2]. Hydrogen storage refers to that compression of hydrogen gas volume, a volume of $11\ m^3$ can store 1 kg hydrogen gas at 25℃ and 1 bar pressure [2]. Generally, hydrogen gas could be stored in a physical or chemical ways [3], such as high-pressure gas cylinders [2], liquid hydrogen [4], and solid hydrogen storage materials [5]-[7] (e.g., metal hybrids and organic-inorganic framework), etc. In the last few years, a large amount of studies and news focus on developing cost-effective hydrogen storage methods with a high gas capacity. Instead of storing hydrogen in the dangerous high-pressure and weighty tank, David Milstein and his colleagues [8] developed a soluble ruthenium catalyst with an organic ligand, a simple organic chemical system, to store and release hydrogen. However, its overall efficiency needs to be further improved since the reaction time is not short enough. Though the metal-organic frameworks (MOFs) are widely investigated for the hydrogen storage application and possess the potential to surpass the capacities of high-pressure tank, few studies have identified the optimal materials or found a benchmark for hydrogen storage due to the large quantity of MOFs studied previously [9]-[13]. Alauddin et al. computationally screened nearly 500,000 compounds to find a

benchmark, at around 40 g $H_2\ L^{-1}$, for hydrogen storage materials [14]. Therefore, the further efforts need to be dedicated to exploring and finding the suitable hydrogen storage materials with a higher capacity.

Besides considering hydrogen storage materials, hydrogen also can be stored in the indirect hydrogen storage media, such as ammonia, methane, methanol and ethylene glycol [21]-[23]. Among them, only ammonia can provide clean energy to electric vehicles without discharging carbon oxide to the atmosphere, possessing a higher energy density than those compressed hydrogen [15]. According to a report in 2019, only 1 % of global emissions were responsible by ammonia, but 17 % of all chemical and petroleum energy was taken up by the ammonia market. It is safe to say that the ammonia is an ideal candidate for green fuel. Japan, a country short of natural energy resource, has considered the ammonia as the potential alternative hydrogen energy carrier. For example, the Japan Science and Technology Agency (JST) plans to form an ammonia value chain which could significantly promote the status of Japan in the production and usage of ammonia worldwide. On the other hand, the IHI company worked with Tohoku University to invest $ 8.8 M on setting up ammonia and methane mixed fueled turbine in 2017 [16].

Ammonia, as a potential energy carrier, has several merits on its production, transportation and safety over other energy sources. The technologies of ammonia synthesis and transportation have been industrialized and widely used in the production of nitrogenous fertilizer. The earliest ammonia production method was known as Haber-Bosch process [17], which can synthesize ammonia (NH_3) from hydrogen (H_2) and nitrogen (N_2) with the presence of iron at high temperature and pressure. However, the Haber-Bosch process is not green at all, since it generates a large amount of carbon dioxide while separating hydrogen from natural gas and melding the hydrogen and nitrogen. To minimize the carbon emissions, novel ammonia synthesis routes have been developed. Yara, the biggest company in the

world to produce ammonia, recently decided to reduce fossil fuel consumption via transforming the first step of Haber-Bosch process toward green, instead of using the natural gas. The total carbon dioxide emissions were cut roughly in half through converting ammonia plants from natural gas to renewable power, like PEM electrolysis and solar power [18]. Unlike Yara's improvement for Haber-Bosch process, MacFarlane developed a reverse fuel cell, using electricity from solar cell and wind plant to drive the reaction between nitrogen and water that synthesis ammonia, which is an precisely zero carbon emission method [19]. Compared with hydrogen, ammonia is inflammable in the air; also a lower overall cost and safety could be guaranteed when it stored in metal ammines ,e.g., $Mg(\mathrm{NH_3})_6Cl_2$ [20]-[21].

As the advantages of ammonia discussed above, more importantly, ammonia can be a potential fuel candidate for fuel cell technology [24]. According to various research on DAFCs in recent years, ammonia can power fuel cells via ammonia itself or supplying hydrogen produced by ammonia thermal decomposition to fuel cells (indirect ammonia fuel cells) [25]. The latter one is ideal for low-temperature proton exchange membrane fuel cells, the acid Nafion membrane, however, is not compatible with direct ammonia fuel, due to the reaction between ammonia and acidic Nafion membrane, also the poison effects of ammonia on Pt/C catalysts [26]. Before the fuel cell operation, the hydrogen decomposed from ammonia requires an additional cracking process, which significantly increases energy input and overall costs. While the former one is more efficient, the electricity generation directly from ammonia, it is suitable for application of alkaline anion exchange membrane fuel cells (AEMFCs) [26]. With the assistance of a grant from the REFUEL program of the Advanced Research Projects Agency-Energy (ARPA-E), Professor Yushan Yan at University of Delaware, demonstrated a peak power density of 135 mW cm^{-2} for a novel DAFC which employed hydroxide exchange membrane and non-platinum catalysts in 2019 [24]. Besides the low temperature AEM-DAFCs, there is a high temperature SO-DAFC offering a better

performance, even similar to pure hydrogen fuel cells [27]. When the ammonia is directly infused into a high temperature SO-DAFC, the ammonia decomposition reaction will absorb heat to cool down the whole system, and the entropy gains, which means the high temperature could enhance the performance of DAFC. Also, other fuels like methanol used in SOFCs may lead to carbon poisoning on anode [28]. Therefore, ammonia as the direct fuel may be a better choice for SOFCs; however, the high-temperature SO-DAFCs need a preheat treatment process before the fuel cell operation. It is more suitable for the stationary energy system, instead of automotive applications. Japan is a country intensively developing renewable energy for its industrial and residential usage. Moreover the IHI, a Japanese manufacturing firm, obtained 1-kW class power from a high temperature DAFC, which could possibly replace those facilities using natural gas in the future [29].

This article will introduce low temperature AEM-DAFCs first and emphasize its development on the electro-catalysts (platinum-based and non-platinum-based catalysts) and AEMs for DAFCs. The recent progress on high temperature SO-DAFCs is summarized as well, and the discussion regarding the remaining challenges and future perspectives of DAFCs is attached in Section 5. Also, Figure. 2 provides a graph for ammonia production and application.

2. Scope and Significance of Article

The ammonia as a potential fuel candidate for the fuel cell application, the studies on DAFCs have enjoyed their popularity since the 1960s, the first alkaline electrolyte fuel cells fed by ammonia was proposed. However, the low-temperature AEM-DAFCs were not gained much attention at the beginning, and most of researches were focused on the high temperature SO-DAFCs, since the inferior performance of the low temperature AEM-DAFC resulted from the low catalytic activity of electro-catalysts and difficulty of ammonia oxidation at low temperatures. Until 2010, a few researches started applying the novel electro-catalysts and

suitable hydroxide membranes to low temperature AEM-DAFCs. For instance, Lan and Tao developed a low temperature AEM-DAFC with nickel anode and MnO_2 cathode [55]. Shohei demonstrated three distinct viable catalysts (Pt/C, Pt-Ru/C, and Ru/C) for low temperature AEM-DAFCs [48]. Unlike previous reviews on DAFCs that spent tremendous efforts to describe the development of high temperature SO-DAFCs , the significance of this review would be an enrichment of a timely and comprehensive review for the development of low temperature AEM-DAFCs. The low temperature AEM-DAFCs part in this review not only clearly reveals the ammonia oxidation mechanism and effect of each component on the fuel cell performance, but also provides possible future research directions from perspectives on materials design for electrode catalysts and AEMs, respectively. On the other hand, this review also is a supplement of high temperature SO-DAFCs for previous reviews. For instance, more possible research directions for high temperature SO-DAFCs are proposed 咱不是专家， 不要用这个词，咱也就是总结 in this review based on recent important progress on the long-term operation stability and efficient catalysts for ammonia decomposition, while research directions suggested in previous reviews were more focused on the effects of different solid electrolyte and electrolyte thickness 这两个方向太小.

3. Low temperature AEM-DAFCs

Compared with hydrogen, ammonia is more energy-efficient, lower production cost and easier to transport. It has attracted many researchers' interests to study ammonia fed fuel cells in the past decades. It is reported that the earliest one alkaline electrolyte fuel cells fueled with ammonia was studied in the 1960s. Cairns and Simons used ammonia as a fuel to operate the fuel cell with a KOH solution electrolyte [30]. Hejze et al. developed a DAFC with the molten hydroxide NaOH/KOH operated from 200 ℃ to 450 ℃, which employed nickel as cathode and anode to achieve a power density of 40 mW cm^{-2} at 450 ℃ [31]. Yang et al. investigated a DAFC with a molten NaOH/KOH electrolyte, and the platinum was used

as electrodes. The fuel cell exhibited a peak power density of 10.5 mW cm^{-2} at 200 ℃. While the peak power density was increased to 16 mW cm^{-2} at 220 ℃. In this study, Pt has effects on ammonia oxidation in a molten NaOH/KOH electrolyte, which means the Pt could be used as the anode in DAFCs [32].

3.1 Working principle of low temperature AEM-DAFCs

As shown in Figure. 1, the low temperature AEM-DAFCs usually supply air and water vapor into cells at the cathode, and the oxygen with react with water in the air to form hydroxide ions. As the alkaline membrane employs the exchange of anions, those hydroxide ions travel to the anode side through the membrane. While the ammonia is diffused into anode side, it will react with those hydroxide ions in the anode catalyst layer to form nitrogen and water molecules. As shown in reactions below, electrons will be consumed when hydroxide ions form at the cathode side, while the electrons will be produced when ammonia oxidizes at the anode side. Thus, the electric current will form an external electrical path. All reactions for low temperature AEM-DAFCs are shown below [33]:

Reaction at anode: $2NH_3 + 6OH^- \rightarrow N_2 + 6H_2O + 6e^-$ E^o_{298K} = - 0.77 V (1)

Reaction at cathode: $\frac{3}{2}O_2 + 3H_2O \rightarrow 6OH^- - 6e^-$ E^o_{298K} = + 0.40 V (2)

Overall reaction: $2NH_3 + \frac{3}{2}O_2 \rightarrow N_2 + 3H_2O$ E^o_{298K} = + 1.17 V (3)

In general, the low temperature AEM-DAFCs are operated at a temperature range from 25 ℃ to 100 ℃. Instead of cracking ammonia to form hydrogen as the fuel, the ammonia fueled in the anode could react directly with hydroxide ions through the AEM, which significantly increase the energy efficiency and reduce the system cost. In addition, this type of fuel cell is one of ideal candidates for future automotive applications, due to the lower cost and suitable operating temperature.

3.2 Development of low temperature AEM-DAFCs

Since the first generation of ammonia fuel cells was reported in the 1960s, DAFCs have been through much progress on electrode materials and electrolyte membranes [41]-[60]. Due to the unique alkaline operating environment within the low temperature AEM-DAFCs, more and more nonprecious metal electro-catalysts were investigated as the potential electrode materials [24],[55]-[61]. Also, efforts have been dedicated to enhancing the Pt-based catalyst utilization efficiency for the ammonia oxidation reaction (AOR), like incorporating Pt catalyst with catalytic metals to alleviate the poisoning effects of ammonia intermediates adsorbed on the Pt based catalyst surface [41]. In addition, the high-performance AEM was designed to accommodate with chemical degradation caused by the degradation of cationic groups [109]. Therefore, the low temperature AEM-DAFCs may be an ideal energy-dense, affordable and carbon-free power source for application of automotive and transportation [24],[60].

3.2.1 Development on the electro-catalysts for ammonia oxidation in alkaline media

• The mechanism of the AOR on Pt and other noble metals

As ammonia is a hydrogen-rich fuel for various promising applications, the mechanism of AOR has been widely investigated [34]-[41]. Most of previous studies involved using platinum as the anode materials and identifying the suitable experimental condition for the AOR. In this case, the oxidation mechanism on the platinum surface has been well understood. In addition, the oxidation mechanism on platinum could be extended to other noble metals. Ideally, NH_3 was proposed to convert to N_2 without further oxidation to nitrate ions. However, an early study on the electrochemical oxidation of ammonia conducted by Muller, the ammonia was electrolyzed with a platinum electrode in a NaOH solution. It turns out that the oxidation products include nitrogen and nitrate ions [34].

$$NH_3 + 7OH^- \rightarrow NO_2^- + 5H_2O + 6e^- \quad (4)$$

$$NH_3 + 9OH^- \rightarrow NO_3^- + 6H_2O + 8e^- \quad (5)$$

The subsequent studies regarding the ammonia oxidation indicated that the anode potential might be related to ammonia over-oxidation to nitrogen oxides. Katan and Galiotto [35] electrolyzed 3 M ammonia in KOH solution in a fuel cell, and the anode was prepared with the platinum black. When the current density from 10 to 100 $mA\ cm^{-2}$ was applied, the gas produced from the ammonia oxidation was pure nitrogen, corresponding to the anode potential range from -0.31 to -0.11 vs SHE. Further, Endo and Katayama [36] provided evidence for potential related ammonia over-oxidation by employing the rotating disk electrode to study the AOR. In their study, there is a water oxidation potential (the oxidation begins at $\sim +0.6\,V$ vs. Ag/AgCl at RRDE), which includes the nitrogen produced from ammonia and oxygen produced from water. In this water oxidation region, the cross-combination product NH_2OH was formed due to the ammonia and water simultaneous oxidation, then the further oxidation products were released, such as NO_2^- and NO_3^-.

$$NH_3 \rightarrow\rightarrow NH_2, NH \rightarrow\rightarrow N_2H_y \rightarrow\rightarrow N_2 \quad (6)$$

$$H_2O \rightarrow OH \rightarrow H_2O_2 \rightarrow\rightarrow O_2 \quad (7)$$

$$NH_3, H_2O \rightarrow\rightarrow NH_2, OH \rightarrow NH_2OH \rightarrow\rightarrow NO_2^-, NO_3^- \quad (8)$$

In later studies, the development of differential electrochemical mass spectrometry (DEMS) revealed the mystery of potential related ammonia oxidation, which could be used to identify intermediate of continuous faradaic reactions [37]. The DEMS proved that the elemental nitrogen was the sole product when the anode potential was below 0 V vs. SHE. While the nitrite and nitrate ions were detected at more positive potentials. The DEMS-CV experiment was conducted by Wasmus to investigate the ammonia oxidation at platinum black in 0.5 M KOH solution [38]. The study confirmed that the nitrogen was the exclusive product at potential less than 0.7 V vs. RHE, and NO, and nitrate ions were formed at anode potential larger than 0.8 V vs. RHE.

After figuring out potential related ammonia over-oxidation, the platinum served as the most widely used electro-catalyst for the AOR. However, the platinum suffers from deactivation effects of strongly adsorbed reaction intermediates. As Gerischer and Mauerer [39] uncovered the mechanism of AOR regarding the theory of production of poisoning species on the platinum surface. According to the recent study on the mechanism, the progressive process of ammonia dehydrogenation could produce surface adsorbed ammonia intermediates ($NH_{x,ad}$) until the N_2H_{ad} is formed. The final step is the dehydrogenation of N_2H_{ad} to yield N_2 [41].

$$NH_{3,ad} + OH^- \rightarrow NH_{2,ad} + H_2O + e^- \quad (9)$$

$$NH_{2,ad} + OH^- \rightarrow NH_{ad} + H_2O + e^- \quad (10)$$

$$2NH_{ad} \rightarrow N_2H_{2,ad} \quad Rate\ limiting\ step \quad (11)$$

$$N_2H_{2,ad} + OH^- \rightarrow N_2H_{ad} + H_2O + e^- \quad (12)$$

$$N_2H_{ad} + OH^- \rightarrow N_2 + H_2O + e^- \quad (13)$$

During the AOR process, the fully dehydrogenated adsorbate (N_{ad}) is inert for N_2 formation. and it is a poisoning species on electrodes, since the N_{ad} adsorbed on the catalyst surface would block anion OH^- adsorption.

Besides the platinum metal as the electro-catalyst for the AOR, other noble metals and transition metals also possess the similar oxidation mechanism with Pt. Instead of using pure noble metal for the AOR, alloying with another transition metal is the most common strategy [52]. Among various metals, only Pt and iridium (Ir) showed a steady-state activity to nitrogen formation. Other transition metals (Ru, Rh, Pd) may not contribute to the nitrogen formation, since the intermediate dehydrogenated adsorbate ($NH_{x,ad}$) produced during the AOR tend to form more stable atomic nitrogen. In addition, like adsorption of N_{ad} on platinum, de Vooys proposed that N_{ad} has poisoning effects on transition metals for AOR, such as Pt, Ru, Pd, and Ir. The adsorption strength for N_{ad} is Ru $>$ Rh $>$ Pd $>$ Ir $>$ Pt $\gg$

Au, Ag, Cu, the stronger adsorption of N_{ad} leads to a worse catalytic activity. Although the noble metals (Au, Ag) and copper have a lower adsorption of N_{ad}, they are inactive for the selective oxidation to N_2. Among these single metals, the Pt is the most active one for AOR [40],[42]. Interestingly, considerable evidence [43] have indicated that the AOR on the Pt surface is sensitive to different catalyst structure. It turns out that the Pt (100) performed a higher oxidation current and nitrogen evolution than Pt (111) and Pt (110), as shown in Figure 3. Although the ammonia as a promising hydrogen rich fuel, and the AOR mechanism has been extensively studied, few single metal catalysts are suitable for the AOR. Previous investigations have demonstrated that the AOR catalytic activity of transition metal group (Ru, Rh, Pd, Ir, Pt) would be significantly influenced by the adsorption of N_{ad}, also the single noble metals are inactive for the selective oxidation to N_2. Therefore, further efforts need to be spared on the development of high catalytic activity catalysts for the AOR with low adsorption of N_{ad}.

• **Development of Pt-based alloy electro-catalysts for the AOR**

Many studies on using Pt electro-catalyst for the ammonia oxidation under the alkaline electrolyte environment have been reported [34]-[41]. However, pure Pt metal catalyst requires a cost, and its activity still suffers from poisoning effects of the adsorption of N_{ad}. Aiming to improve the catalytic activity, some binary electro-catalysts have been studied in the past few years [45]-[49]. Kazuki Endo et al. enhanced the electro-catalytic activity via incorporating Ir and Ru separately with pure Pt metal catalyst. Compared with the lowest ammonia oxidation potential (0.1V) on pure Pt catalyst, the binary catalyst started the dehydrogenation steps of ammonia at a lower potential (around -0.6V) [44]-[45]. Lomocso et al. demonstrated Pt-Ir based catalyst has a higher AOR catalytic activity compare to Pt-Pd and Pt catalyst [46]. Recently, a low temperature AEM-DAFC with electro-catalysts of Pt-Ir/C and Pt/C was investigated. It was shown that using anode of Pt-Ir/C with fuel NH_4OH

5.0 $mol\ L^{-1}$ in KOH 1.0 $mol\ L^{-1}$ at 40 ℃ received a 48% and 70% higher peak power density, instead of using Pt/C and Ir/C binary catalyst [47]. In another study, the catalytic activity of three distinct catalysts (Pt/C, Pt-Ru/C, and Ru/C) was investigated via the characterization of low temperature AEM-DAFCs. The cyclic voltammetry over three catalysts for the AOR indicated that the initial ammonia oxidation potential from the highest to the lowest was Pt-Ru/C (0.37V), Pt/C (0.54V), Ru/C (0.08V), which is also the order of catalytic activity [48]. Assumpcao et al. investigated a low temperature AEM-DAFC employed PtRh/C and Pt/C electro-catalysts, respectively. The operating temperature was fixed at 50℃ and fueled with ammonia hydroxide. The open-circuit voltage (OCV) of 0.3 V and 0.2 V were applied on Pt/C and Pt/Rh/C electro-catalysts, respectively. The Pt-Rh/C electrocatalyst with a Pt/Rh ratio 90:10 showed a 60% higher power density than pure Pt catalyst within DAFC performance test [49]. Following the similar track, the metal oxides, especially rare earth oxides ($CeO_2, Y_2O_3, La_2O_3\ and\ Sm_2O_3$) modified Pt catalyst for AOR was studied. The results indicated that the metal oxide additive enhanced the supply capacity of OH^- adsorption to the active sites on Pt, and the CeO_2 showed the highest current increase [50]. A recent study proposed that SnO_2 modified Pt electrocatalyst was suitable for low temperature AEM-DAFCs. In the experiment, the cathode employed the commercial Pt/C catalyst with a loading of 0.4 $mg\ cm^{-2}$, and SnO_2-Pt/C catalyst as the anode. The fuel cell was operated at 50 ℃, the anode was supplied with humidified ammonia, and the cathode was supplied with oxygen, both of which at the same flow rate of 100 mL min^{-1}. The SnO_2-Pt/C exhibited a more stable chemical stability in alkaline environment and a higher current density than Pt/C did [51].

On the other hand, introducing the noble metals (Au, Ag, Cu) to pure Pt not only can improve the performance, also decrease the poisoning effects caused by N_{ad}. The Pt-Au/C electrocatalyst with a distinct Pt/Au atomic ratio was applied on low temperature AEM-

DAFC application. The experiments were conducted in a single cell with an active area of 5 cm^2 . The fuel, NH_4OH in 1.0 mol L^{-1} KOH, was supplied with a flow rate of 1mL min^{-1}, and oxygen with a flow rate of 150 mL min^{-1}. PtAu/C (50:50) and PtAu/C (70:30), Au/C and Pt/C was used as the anode, respectively. It was shown that the Pt-Au/C (70:30) obtained the best performance, achieving a 20% higher current density and a 60% higher power density than Pt/C catalyst did in DAFC. More importantly, the more stable current density reduction of PtAu/C (70:30) in chronoamperometry indicated that Au could weaken the poisoning effects from N_{ad} species on the catalyst surface, facilitating the AOR [52].

It is proposed that several ternary electro-catalysts introduced the third type of metal also have a performance enhancement [53][54]. Pt-Ir-Rh catalyst on carbon fiber substrate was used as the electrode. Compared with binary Pt-Ir catalyst, the Pt-Ir-Rh showed a high Faradaic efficiency of 91.81% for ammonia electrolysis at low concentration of ammonia [53]. Similarly, another metal Zn was incorporated into Pt and Pt-Ir electrodes, the CV studies revealed that Pt-Zn and Pt-Ir-Zn have a more active AOR compared to those Pt and Pt-Ir electrodes. By adding Zn to Pt-Ir, the lowest onset AOR potential decreased from 0.41 V to 0.3 V. The Tafel plots showed that the exchange current density increased from $1.2 \times 10^{-8}\ A\ cm^{-2}$ to $4.3 \times 10^{-8}\ A\ cm^{-2}$ after combining Zn with Pt-Ir [54].

To enhance the catalyst activity, some binary electro-catalysts and ternary electro-catalysts were introduced for the AOR and low temperature AEM-DAFC applications. Since the Pt is the most active single metal for the AOR [42], the binary strategy usually incorporated Pt with another transition metals (Ru, Rh, Pd, Ir) or noble metals (Au, Ag) to further improve the catalytic activity and to alleviate poisoning effects from the adsorption of N_{ad}. In addition, incorporating third type metal based on those binary electro-catalysts also proves a performance enhancement. However, the optimal electro-catalyst for the AOR among those binary and ternary combined catalysts is hard to be identified, due to the various experimental

conditions. More systematic studies should be conducted to identify the optimal platinum based electro-catalyst for the AOR in the future.

•Development of non-platinum group metal electro-catalysts

Except for introducing other metals or modifying the Pt metal to improve catalytic activity for the AOR in DAFCs, using platinum-free electro-catalysts is an alternative way to explore [24],[55]-[61]. Lan and Tao reported that ammonia can be used as fuel for low temperature AEM-DAFCs employed nickel as anode and MnO_2 as cathode. Two different cells performance were compared, one cell was fabricated with a MnO_2/C cathode, PtRu/C anode, and the other used Gr decorated Ni (CDN) as the anode, and MnO_2/C as the cathode. 35 wt. % aqueous ammonia solutions, ammonia gas and oxygen/air were fueled for the fuel cell testing. The results demonstrated that nano-sized nickel catalysts was more preferred than PtRu/C due to a higher catalytic activity toward AOR. More importantly, their DAFC achieved a slightly higher OCV and peak power density than hydrogen fed fuel cell with the same catalyst [55]. Recently, the iron could be a potential catalyst for AOR, due to the similar onset potential of the AOR on Fe and Pt, although the iron has a tendency of corrosive dissolution. During the process, the iron nitride film on iron catalyst surface is resistant to dissolution [56].

It was demonstrated that NiCu layered hydroxides (LHs) could be another potential electrode for low temperature AEM-DAFCs. Compared with the commercial Pt/C and bare nickel hydroxides catalyst for AOR, the current density of NiCu layered hydroxides is seven time of that for bare $Ni(OH)_2$. It also has a superior AOR activity, which could be attributed to the synergistic effect between Cu and Ni. However, modified the bare $Ni(OH)_2$ catalyst with Co, Zn, Fe or Mn, the activity of $Ni(OH)_2$ would be lower rather than enhanced [57]. Further, using NiCu as the anode materials for low temperature AEM-DAFCs application has been demonstrated by Zhang et al. In the study, the different mass ratios of NiCu electro-catalyst

supported on nanotubes (CNTs) were prepared via hydrothermal method. Then the ammonia-air microfluidic fuel cell was fabricated to characterize the electrochemical performance for NiCu/CNTs electro-catalyst, which indicated that 50 wt. % $Ni_{50}Cu_{50}$/CNTs was most suitable one due to its 43% higher peak power density compared to Ni electrodes, as shown in Figure. 4 a,b,c. The operating temperature was set at 25℃ with a fuel flow rate around 500 μL min^{-1}, and loading of 2 $mg\ cm^{-2}$ of commercial Pt was used as the cathode [58]. Similarly, Zou et al. also reported a low temperature AEM-DAFC study using NiCu/C as anode with loading of 2.5 $mg\ cm^{-2}$, but applying single-phase perovskite oxide $SrCo_{0.8}Cu_{0.1}Nb_{0.1}O_{3-\delta}$ as the cathode instead of commercial Pt catalyst. As shown in Figure. 4.d, the peak current density and power density of 5 $mA\ cm^{-2}$ and 0.25 $mW\ cm^{-2}$ were achieved [59].

As the considerable studies demonstrated that platinum-free electro-catalysts, such as Fe, NiCu/C, etc, could accommodate the alkaline environment within the low temperature AEM-DAFCs, also exhibit a comparable even higher AOR catalytic activity than those platinum-based catalysts. The presence of platinum-free electro-catalysts may be the key for the future development of AOR electro-catalysts and reducing the cost of low temperature AEM-DAFCs. However, those low temperature AEM-DAFCs employed platinum-free electro-catalysts did not gain a satisfied performance yet, which may be resulted from the various cell operating conditions (like temperature, PH, membrane electrolyte, etc.), or the limited catalytic activity for the platinum-free catalysts. Further exploration on the development of platinum-free catalysts and performance enhancement for the low temperature AEM-DAFCs would be necessary.

•Single-cell performance of low temperature AEM-DAFCs

Although many studies have been dedicated to low temperature AEM-DAFCs, reported peak power density of DAFCs still was around 10 $mW\ cm^{-2}$ or less. Until recently, a promising

peak power density of 420 $mW\ cm^{-2}$ was reported by Gottesfeld, the DAFC was operated at 100 ℃ with an anode of platinum electro-catalyst and a cathode of platinum-group-metal-free electro-catalyst [60]. In addition, Zhao demonstrated a high-performance DAFC employing a non-platinum-group-metal as the cathode, and the Poly (aryl piperidinium) (PAP) as the membrane electrolyte. A peak power density of 135 $mW\ cm^{-2}$ was achieved at 80 ℃ [24]. More interestingly, Kumar et al. reported a high-performance DAFC used the cow dung based compost as the catalyst for cathode. The results exhibited a peak power density of 108 $mW\ cm^{-2}$, and the cell had negligible de-activation of electro-catalyst after 12 h continuous operation [61]. The previous studies on performance of low temperature AEM-DAFCs were summarized in Table 1. Among those data in Table 1, it is easy to find that a peak power density of 420 $mW\ cm^{-2}$ reported by Gottesfeld [60] and a peak power density of 135 $mW\ cm^{-2}$ reported by Zhao [24] are far higher than others. Their desirable cell performance could be attribute to higher cell operating temperature and hydroxide concentration, since the rotating disk electrode (RDE) results demonstrated that higher cell operating temperature would substantially increase the AOR kinetics and DAFC performance with PtIr/C electro-catalyst, also the higher hydroxide concentration within the fuel cell could decrease the onset potential for the AOR [24]. Therefore, it could be inferred that for other active AOR catalysts, including the platinum-free catalyst, the cell operating temperature and hydroxide concentration would be two key factors that influence the catalytic activity and low temperature AEM-DAFC performance. But it is still not clear that how the influence varied with different catalysts. In addition, the ammonia crossover is inevitable for the low temperature AEM-DAFC, for the common platinum-based catalyst as cathode, the activity of the ORR at cathode side would significantly decrease due to the surface poisoning from the AOR, consequently, a lower fuel cell performance [24],[48]. However, few studies on low temperature AEM-DAFCs have considered the effects of ammonia crossover on platinum-

free catalysts at the cathode. In conclusion, the investigation of platinum-free electro-catalyst for low temperature AEM-DAFCs still was at an early stage, its maximum current density and peak power density are still lower than those hydrogen fed fuel cells. The further researches are needed to conduct on effects of cell operating temperature and hydroxide concentration on the AOR activity of distinct platinum-free catalyst anodes. On the other hand, the future development of platinum-free catalysts for the cathode with a high ORR activity needs to consider the issue of ammonia cross-over, if there will be the formation of surface poisons on the catalyst at the cathode. Ideally, preparing a cathode platinum-free catalyst with zero AOR activity but with a high ORR activity, or developing a membrane with a super low ammonia permeation could minimize the effect of ammonia cross-over.

3.2.2 Progress on alkaline AEM for low temperature AEM-DAFCs

Generally, the AEM was composed of a main chain and many side chains, where the main chain is just a polymer backbone and the attached side chains serve as cationic groups. Those cationic groups have effects on transportation ability of hydroxide ions. Since the chemical composition of the AEM is related to its properties and performance, a wide range of study were conducted on AEMs based on distinct polymer backbones and functional groups. The polymer backbones of membranes usually include poly (vinyl alcohol) (PVA), poly (arylene ether), poly(2,6-dimethyl-1,4-phenyleneoxide) (PPO), poly(tetrafluoroethylene) (PTFE), and polysulfones [62]-[66]. On the other hand, there are two common types of functional groups attached on polymer backbones, i.e., quaternary ammonium (QA) and imidazolium [67]-[69]. As the low temperature DAFCs require an alkaline operating environment, the alkaline AEM becomes a necessary part. It does play a significant role on AOR, such as transporting hydroxide ions and separating different phases of fuel. However, few studies have focused on improving the ionic conductivity and mechanical strength of alkaline AEMs, especially for the application of low-temperature AEM-DAFCs. Fortunately, previous abundant exploration

on high-performance alkaline AEMs indicated a promising track to identify the potential alkaline AEM for low temperature AEM-DAFC applications.

•Hydroxide-ion conductivity

Besides the effects of electro-catalysts, the performance of low temperature AEM-DAFCs was highly dependent on the membrane electrolyte. The ionic conductivity and membrane swelling degree, are always two most important factors to qualify a membrane. When it comes to the ionic conductivity, ammonia fuel cells using alkaline AEM to avoid precipitates formation (K_2CO_3, Na_2CO_3), but the membrane still would be able to react with CO_2 to form CO_3^{2-} ions, which significantly reduces OH^- ion conductivity [77]. Thus, figuring out a way to increase the ionic conductivity could be a big step for fuel cell performance improvements. Previous studies have shown that the ionic conductivity for AEMs has a close connection with exchange capacity (IEC) and water uptake (WU). A higher IEC may result in an increased WU of the membrane and hydrophilic domain connectivity, therefore, a lower energy barrier required by the hydroxide-ion transportation, which means a higher ionic conductivity [62]-[69].

Various approaches for the enhancement of the hydroxide-ion conductivity were reported recently [70]-[74]. The most common one is to modify polymer side chains, since the cationic groups on the side chains are related to mobility of OH^- ions through membrane. Li et al. prepared an anion conductive electrolyte for alkaline fuel cell via synthesizing a series of quaternized poly (2,6-dimethyl phenylene oxide) (PPO) containing long alkyl side chains pendant to the nitrogen-centered cation. It was found that there is a hydrophilic-hydrophobic separation induced from the long alkyl side chains, which could enhance the ionic conductivities. Up to 16 carbon atoms of one long alkyl side chain based on PPO backbone exhibited a high hydroxide-ion conductivity around 21 mS/cm and an IEC at 1.6 meq/g [70]. In addition, introducing multiple side chains also could increase hydroxide ion conductivity.

Wang et al. fabricated a high ionic conductivity AEM via introducing multiple QA groups to poly (arylene ether sulfone)s (PAES as the backbone), which refers to membrane with PAES-Q-xx chemical composition. It was proved that PAES-Q-xx membrane has IEC values around 1.65-2.36 meq/g, and its highest ionic conductivity was 82 mS/cm at 80 ℃ [71].

Following the similar track, the high hydroxide-ion conductivity AEMs were utilized for low temperature AEM-DAFC applications, via modifying the cationic groups on the side chains. For instance, the commercial fumapem FAA AEM (Fumatech, OH^-form) is a hydrocarbon membrane with the chemical composition of the aminated poly arylene chloride. More specifically, for the QA based AEM, its hydroxide-ion conductivity depends on the quaternizing functional groups [75][76]. Zou et al. developed a low temperature AEM-DAFC with the FAA AEM, and the NiCu/C, $SrCo_{0.8}Cu_{0.1}Nb_{0.1}O_{3-\delta}$ catalysts were used as anode and cathode, respectively. The maximum current density and power density of 5 $mA\ cm^{-2}$ and 0.25 $mW\ cm^{-2}$ were observed at 25 ℃ [59]. It was proposed that the commercial AEM (A201, Tokuyama Co.), another type of QA based AEM, was suitable for low temperature AEM-DAFC applications. Okanishi et al. reported a low temperature AEM-DAFC composed of AEM (A201, Tokuyama) as the electrolyte membrane, the SnO_2-Pt/C catalyst as the anode, and commercial Pt/C as the cathode. The maximum current density around 0.04 $mA\ cm^{-2}$ was achieved at an operation temperature of 50 ℃ [51]. Another study on the effect of carbonate ion species in low temperature AEM-DAFC also employed AEM (A201, Tokuyama) as the membrane electrolyte [77]. Recently, a new generation of AEM, Poly (aryl piperidinium) (PAP), was prepared. By increasing the number of cationic groups on the polymer backbone, this kind of membrane gains higher hydroxide ion conductivity (175 $mS\ cm^{-1}$ at 80 ℃), also having a perfect chemical stability (no obvious degradation in 1 M KOH at 100 ℃ for 2000 h) and an optimal mechanical strength [78]. At the same year, the PAP membrane was applied for a high-performance low temperature AEM-DAFC. A

platinum-free electro-catalyst for cathode made by Acta (Acta 4020, 3.5 wt. % carbon supported transition metal), possessed a better ORR activity than the Pt/C did while the ammonia cross-over to cathode. The PAP membrane and the novel platinum-free catalyst used in this low temperature AEM-DAFC, which enabled the operation temperature as high as 80 ℃ and achieved a peak power density of 135 $mW\ cm^{-2}$ [24].

Beyond the methods of improving ionic conductivity mentioned above, Hou et al. reported Nafion@ 112 membrane modified with KOH solution may be applied for low-temperature AEM-DAFC applications, since the Nafion@ 112 membrane doped with KOH solution gains a higher ionic conductivity under alkaline environment. Also, the Nafion@ membrane exhibited a better chemical and thermal stability [79]. Recently, Assumpcao et al. conducted two experiments to demonstrate the modified Nafion@ membrane could be applied for low temperature AEM-DAFC, the peak power density of 5.37 $mW\ cm^{-2}$ and 4.17 $mW\ cm^{-2}$ at 50 $℃$ and 40 $℃$ were obtained, respectively [47],[49]. But their studies did not mention the ionic conductivity results for the modified Nafion@ membrane.

In summary, modifying the cationic groups on side chains of polymer, or introducing multiple cationic groups on polymer would be two common ways to enhance the ionic conductivity for AEMs. However, a high IEC and WU for a high ionic conductivity AEM may lead to an extensive membrane swelling, which significantly increases the ohmic loss during the fuel cell operation. Further researches on the development of AEMs would be required to maintain a high ionic conductivity but with a low swelling degree. More importantly, most of previous studies on high ionic conductivity AEMs were focused on those fuel cells fueled with hydrogen. Except for few investigations on the commercial AEM (A201, Tokuyama) and FAA AEM for ammonia fuel cells, more efforts should be dedicated on identifying the recent synthesize AEMs with a higher ionic conductivity for low temperature AEM-DAFC applications. With more different synthesized AEMs trialed for the

low temperature AEM-DAFC, the benchmarks of suitable AEMs for ammonia fuel cells would be progressively set up, providing more perspectives for development AEMs of the low temperature AEM-DAFCs.

•Mechanical strength

Although the ionic conductivity improvement is correlated to an increase of IEC, the mechanical integrity of a membrane could be a challenge at a higher IEC, since the excessive WU results in a membrane swelling and the decline of mechanical strength. In order to address this issue, several studies have been conducted so far [82]-[84]. The first plausible way was to cross-linking the polymer chain, since the mechanical properties of a polymer are highly dependent on the extent of polymer chain entanglement, a high molecular weight membrane usually owns better mechanical properties. At the same time, a higher molecular weight has little impact on water uptake and hydroxide conductivity [80],[81]. And the other alternative method was to design the Nafion-resembling phase-separation structure in AEMs, as shown in Figure 5. Different from the first strategy for cross-linking, the second method was to introduce additional hydrophobic side chains with a moderate IEC to drive the aggregation of hydrophilic domains (corresponding to change form Figure. 5 (a) to (d)). In this case, the moderate IEC can guarantee the low swelling degree, also these hydrophobic side chains will enhance the conduction of hydroxide ions [82].

Alleviating the membrane swelling degree via cross-linking polymer has been applied in low temperature AEM-DAFC applications [24],[55],[85],[86]. Lan and Tao developed a low temperature AEM-DAFC employed chloroacetyl poly (2,6-dimethyl-1,4-phenylene oxide) crosslinked with poly (vinyl alcohol) CPPO-PVA based AEM, since the mechanical strength of CPPO is unsatisfactory, which is hard to form a dense membrane. The DAFC operated with CDN/C anode and MnO_2/C cathode at room temperature, then a peak power density of 16 $mW\ cm^{-2}$ was achieved [55]. Recently, Siddiqui et al. developed cross-linking type

membrane via cross-linking a gel polystyrene with divinylbenzene, and the QA and the ionic form chloride as the functional group. At the ambient operating temperature (25 ℃) and a pressure of 100 kPa (1 bar), the membrane was used in a low temperature AEM-DAFC as the electrolyte, and electrodes employed the 40 wt. % commercial Pt/C catalyst. Fueling with gaseous ammonia, the peak power density around 64 ± 3 m$W\ cm^{-2}$ was achieved [85]. Later, Siddiqui used the same AEM and Pt based catalyst for low temperature AEM-DAFC, a higher peak power density was reported to be 192 m$W\ cm^{-2}$ [86].

As mentioned earlier, a better mechanical strength of an AEM could be achieved via cross-linking polymer chains to obtain a higher molecular weight membrane or introducing additional hydrophobic side chains. However, a high molecular weight AEM requires multiple steps for polymerization and high purity monomers, which means a high production cost. Further studies would be worthful reducing the membrane production cost or exploring alternative ways to improve mechanical strength of AEMs. Despite the improvement has been made on the AEMs mechanical strength, the membrane thickness turns out to be the key factor that requires a further mechanical strength improvement. Because at a given ionic conductivity, a thinner membrane within the AEMFC could suffer less from the ohmic losses during the cell operation [87]. As shown in Figure. 6, the reinforced AEM with 10 μm thickness exhibits the less voltage loss at ohmic loss region than the AEM with 30 μm thickness does. It would be necessary to develop the thinner membrane fabrication method for those AEMs with a good mechanical strength in the future. But simultaneously, the issue of ammonia cross-over would be more severe for a thinner AEM, which may not only poison the cathode catalyst but lower the cell voltage. Therefore, the thinner AEMs with high mechanical strength and low ammonia permeation would be the goal for the future research and development on the membrane for low temperature AEM-DAFCs.

4. High temperature SO-DAFCs

For the DAFCs, another optimal way is to operate the SOFCs with high temperature, which refers to the high temperature SO-DAFCs. Generally, there are proton conducting and anion conducting electrolyte based high temperature SO-DAFCs reported [100]-[108]. In 1980, the first anion conducting type of high temperature SO-DAFC was proposed [88], the fuel cell used Yttria stabilized zirconia (YSZ) as the electrolyte and the platinum as the electrodes to generate electricity and nitric oxide. Although the ammonia was oxidized to nitrogen at the final step, it was found that a few nitric oxides are produced at the anode due to the slow diffusion of O_2 through the electrolyte. There are two options available to reduce the production of NO during the fuel cell operation. The first route is to find the suitable anode materials (Fe or Ni based catalyst, doped $BaCeO_3$ and $BaZrO_3$) to facilitate the decomposition of ammonia, then the hydrogen from ammonia decomposition could directly react with O^{2-} through the electrolyte or transport to cathode to react with oxygen [89]-[92]. In this case, the formation of nitric oxide could be minimized. The other way is to run the DAFCs at the temperature above 500 ℃, since a higher temperature also significantly enhance the ammonia thermal decomposition [93]. Thus, ammonia decomposition has been developed to the first step for anodic reaction for high temperature SO-DAFC applications.

4.1 Working Principle of high temperature SO-DAFCs

Ammonia as a promising energy source, with a comparatively high hydrogen content, can be directly fueled for SOFCs. Base on the different electrolyte, the high temperature SO-DAFCs can be sorted into the proton conducting based SOFC (SOFC-H) and the anion conducting based SOFC (SOFC-O). Although two types of fuel cell have distinct mechanisms, they share the same first reaction step during the fuel cell operation. The hydrogen in the whole reaction comes from the ammonia thermal decomposition.

Ammonia decomposition: $$NH_3 \leftrightarrow \frac{3}{2}H_2 + \frac{1}{2}N_2 \quad (14)$$

For the SOFC-H, the ammonia will decompose to form nitrogen molecule and hydrogen molecule. Then, the hydrogen is oxidized to proton (H^+) with the presence of catalyst. Those protons transfer through the proton conducting electrolyte to the cathode side, where the water vapor produced from the reaction between oxygen and those protons.

Reaction at the anode side: $H_2 \rightarrow 2H^+ + 2e^-$ $E^o_{298K} =$ 0 V (15)

Reaction at the cathode side: $O^2 + 4H^+ + 4e^- \rightarrow 2H_2O$ $E^o_{298K} =$ 1.23 V (16)

For the SOFC-O, generally, the ambient air or pure oxygen is fueled into the cathode side, and hydrogen produced from ammonia thermal decomposition is fed to the anode side. The oxygen will be reduced to oxygen ions, which transports through the anion conducting electrolyte to the anode side, where the water vapor produced from the reaction between hydrogen and O^{2-} ions.

Reaction at the anode side: $H_2 + O^{2-} \rightarrow H_2O + 2e^-$ (17)

Reaction at the cathode side: $\frac{1}{2}O_2 + 2e^- \rightarrow O^{2-}$ (18)

The working principle of high temperature SO-DAFCs, as shown in Figure. 7. Unlike the low temperature AEM-DAFCs, both the SOFC-H and SOFC-O first efficiently crack the ammonia to hydrogen with their high operating temperature (400 ℃ ~ 1000 ℃). The hydrogen is the real fuel for those high temperature SO-DAFCs, also their peak power densities are far higher than those low temperatures, which may attribute to N-H bond breaking under high temperature, a faster reaction kinetics. In addition, their ideal performance indicates a promising future in the stationary energy storage system.

4.2 Performance of high temperature SO-DAFCs

For the SOFC-O, the Samarium doped ceria (SDC) and Yittria stabilized zirconia (YSZ) are two types of oxygen ion conducting electrolyte widely used in past few years [94]-[103]. Fournier conducted study on an intermediate temperature DAFC with the YSZ. In his work, the silver, platinum and nickel cermet were employed as anode respectively to study the fuel

cell performance. It turns out that the nickel based ammonia fuel cell has a higher peak power density than hydrogen fed fuel cell at the 800 ℃ [94]. Zhang et al. reported a high temperature SO-DAFC with the 15 μm thickness YSZ, NiO anode and $La_{0.67}Sr_{0.33}MnO_{3-\delta}$ (LSM) cathode. A peak power density 202 mW/cm^2 was achieved at 800 ℃ [95]. Further, an YSZ electrolyte based high temperature SO-DAFC with nickel anode and YSZ-LSM cathode, exhibiting a peak power density of 526 mW/cm^2 at 850 ℃ [96]. In a recent study, different nickel-based anode materials were studied for high temperature SO-DAFCs with YSZ electrolyte and LSM cathode. It was proved that gadolinia-doped ceria (GDC) blended nickel was more suitable for ammonia fuel cells since the higher catalytic activity than YSZ blended nickel [97]. When the operating temperature was 900 ℃, a peak power density 88 mW/cm^2 was observed for a YSZ electrolyte fuel cell with YSL blended nickel anode and LSM cathode [98]. Compared with the YSZ, the SDC was also served as a better electrolyte in high temperature SO-DAFCs, since SDC has a higher anion conductivity at an intermediate temperature. A peak power density 252.8 mW/cm^2 obtained for a SDC electrolyte (50 μm thick) based fuel cell with Ni-SDC (mass ratio is 65:35) anode and SSC ($Sm_{0.5}Sr_{0.5}CoO_{3-\delta}$)-SDC cathode, the fuel cell was fueled with ammonia at the 700 ℃. However, the peak power density for DAFC still lower than hydrogen fueled one [100]. In addition, a greater peak power density 1190 mW/cm^2 at 650 ℃ were observed, when the DAFC employed SDC electrolyte (10 μm thickness) with nickel anode and $Ba_{0.5}Sr_{0.5}Co_{0.8}Fe_{0.2}O_{3-\delta}$ (BSCF) cathode. However, when the fuel cell was supplied with hydrogen, a greater peak power density of 1872 mW/cm^2 was obtained at 650 ℃ [27]. The same SDC electrolyte and nickel anode were used in another high temperature SO-DAFC, but with different cathode materials (SSC/SDC), obtaining a lower peak power density of 467 mW/cm^2 at 650 ℃ [101].

On the other hand, the SOFC-H have received the similar attention as the anion conducting one, although the SOFC-H have a lower power density. Maffei et al. reported a high temperature SO-DAFC with a gadolinium and praseodymium doped barium cerate electrolyte ($BaCe_{0.8}Gd_{0.15}Pr_{0.05}O_3$, BCGP). A peak power density of 28 mW/cm^2 obtained at 600 ℃ for an ammonia fueled cell employed the NiO-$BaCe_{0.85}Eu_{0.15}O_3$ (NiO-BCE) as anode, platinum as cathode [102]. Similarly, Ma et al. conducted an experiment on high temperature SO-DAFCs used NiO- $BaCe_{0.8}Gd_{0.2}O_{2.9}$ (BCGO) as anode, the $La_{0.5}Sr_{0.5}CoO_{3-\delta}$ (LSCO)-BCGO as cathode, and the BCGO as the electrolyte. In the experiment, the peak power density of 384 mW/cm^2 was found at 750 ℃, which has comparable performance with the fuel cell fed by hydrogen [103]. In addition, different electrolytes BCGP and gadolinium doped barium cerate (BCG) were compared for the performance of high temperature SO-DAFCs. In this study, both anode and cathode were made of platinum, and a 40% higher power density was observed at 700 ℃ when ammonia fuel cell using BCGP electrolyte [104]. In another case, still employing platinum as electrodes, but a 1300 μm thick BCG electrolyte for the high temperature SO-DAFC. A peak power density of 25 mW/cm^2 is obtained at a temperature of 700 ℃ [90]. Xie et al. studied a SOFC-H with the NiO-$BaCe_{0.9}Nd_{0.1}O_{3-\delta}$ (BCNO) anode and $La_{0.5}Sr_{0.5}CoO_{3-\delta}$ cathode. Their DAFCs operated with a 20 μm thick BCNO electrolyte at the temperature of 700 ℃, achieving a peak power density of 315 mW/cm^2 and OCV of 0.95 V, respectively. However, the overall cell performance was still inferior to hydrogen-fueled SOFC [105]. Further, Zhang et al. observed an OCV of 1.1 V and peak power density of 200 mW/cm^2 for a SOFC-H with the BCGO electrolyte, Ni- $Ce_{0.8}Gd_{0.2}O_{1.9}$ (Ni-CGO) anode, and $Ba_{0.5}Sr_{0.5}Co_{0.8}Fe_{0.2}O_{3-\delta}$ (BSCFO)-CGO cathode [106]. Lin et al. studied an anode (NiO-BZCY) supported SOFC-H with $BaZr_{0.1}Ce_{0.7}Y_{0.2}O_{3-\delta}$(BZCY) electrolyte and BSCF cathode. In the study, the fuel cell was fueled with ammonia within a range of temperature (450 ℃-

750 ℃), and a peak power density was identified as 390 mW/cm^2 at 750 ℃ [107]. Recently, the $BaCe_{0.90}Y_{0.10}O_{3-\delta}$ (BCY10) was investigated as the proton-conducting electrolyte for high temperature SO-DAFCs. A peak power density of 216 mW/cm^2 was obtained for the DAFC employed $Ni/BaCe_{0.75}Y_{0.25}O_{3-\delta}$ (Ni/BCY25) as the anode and platinum as the cathode at 650 ℃ [108].

In summary, Table 2 lists the OCV and peak power densities of different high temperature SO-DAFCs operated at various temperatures. As shown in the Table 2, the performance of the SOFC-O is much better than the SOFC-H, which could attribute to different mechanisms and issues regarding to ammonia decomposition and catalysts.

4.3 Catalysts for high temperature SO-DAFCs

To have a better understanding on the relationship between catalyst and performance of high temperature SO-DAFCs, it would be necessary to bring up an introduction on ammonia thermal decomposition. As mentioned before, ammonia thermal decomposition is the first reaction step during the operation of SOFC-H and SOFC-O, providing hydrogen that transports to cathode 氢气到阴极？ to react with oxygen or directly react with O^{2-} through the electrolyte. For high temperature SO-DAFCs, they rely much on the hydrogen fuel from ammonia thermal decomposition during the operation. Theoretically, the performance of high temperature SO-DAFCs will be comparable to those SOFCs fueled with hydrogen, if the ammonia could decompose to hydrogen at a very fast rate. Hence, the conversion percentage and conversion rate of ammonia decomposition will be key points for achieving an optimal fuel cell performance. Chiuta et al. [109] reported that the ammonia thermal decomposition is endothermic and equilibrium limited reaction, and 注意两个别列句子要有连词 its conversion is highly dependent on temperature. They calculated the conversion rate of ammonia decomposition with a temperature range from 250 – 700 ℃, which indicated that the complete ammonia decomposition (> 99 %) could be achieved when temperature above

400 ℃. However, the operation temperature around 400 ℃ is not high enough, since the ammonia decomposition kinetics 这个词好像是单数 at 400 ℃ are quite slow, even though the ammonia conversion is almost complete [25]. On the other hand, the overpotential and theoretical efficiency of SOFCs would decrease at a higher temperature, though a high operation temperature could largely improve the ammonia decomposition. Therefore, operating the SOFC at an intermediate temperature with an active anode catalyst for ammonia decomposition would be a wise strategy.

Many previous works on different catalysts for ammonia thermal decomposition have been extensively explored. Single metal catalyst or compounds, like Ru, Ni, Pt, Pd, Ni-Pt, Ni-Co and Ni-Ru have been studied [110]-[112]. But when we select the suitable one from those catalysts for high temperature SO-DAFCs application, the catalytic activity for ammonia decomposition reaction would be the first thing to consider. Yin et al. [113] and Ganley et al. [114] explored the effects of different active single metal catalysts and different support materials(CNTs, Al2O3) on ammonia decomposition reaction. Their results uncovered the catalytic activity of those catalyst with a following order (Ru > Ni > Rh > Co > Ir > Fe > Pt > Cr > Pd > Cu). Ruthenium Ru 已经算缩写了，不好再用全称 is the most active one among those metal catalysts. However, the balance between cost and catalytic activity would always be significant when applying the suitable catalyst on DAFC applications. Since the ruthenium is more expensive than 比较级 most of catalysts, the less active catalysts (Ni, Co, Fe) with a lower cost compared to ruthenium gain tremendous attention from researchers. As summarized in Table 2, many studies on high temperature SO-DAFCs tend to utilize Ni based catalyst as the ideal candidate for anode materials [95]-[108], which may be attributed to a catalytic activity only less than Ru. For example, Fournier et al. [94] conducted a study on SOFC-O to compare catalytic activity of different catalyst (Ni, Pt, Ag) for ammonia

decomposition. The Ni-based catalyst exhibited the best performance and over 90 % ammonia conversion, especially at 1073 K. In this case, most of previous studies concentrated on the solid electrolyte for DAFCs instead of the further researches on anode catalyst with a higher catalytic activity. And it is also because the solid electrolyte serves as proton conducting materials in DAFC, which is a more crucial factor for performance improvement of DAFC in current stage. Hence, it would be necessary to design high catalytic activity anode catalysts for high temperature SO-DAFCs application.

Herein, this review provides two possible strategies to obtain high catalytic activity catalyst for high temperature SO-DAFC applications. First of all, considering catalysts with bimetallic composition would be a viable way to further enhance the catalytic activity of Ni-based catalyst applied on high temperature SO-DAFCs. Leybo et al. [115] recently developed Ni-Mo nitride catalyst for ammonia decomposition, which achieved almost 100 % ammonia conversion at an intermediate temperature 650 ℃.和之前不一样 Lucentini et al. [116] found that the bimetallic Ni-Ru catalyst supported on CeO_2 has a superior catalytic activity to Ni catalyst supported on CeO_2. The Ni-Ru catalysts even exhibited the 4 times higher ammonia conversion than Ni catalyst at a low temperature 400 ℃. On the other hand, utilizing the Ni based catalyst with nanoparticle size could enhance the catalytic activity. A kinetic study conducted by Zhang et al. [117] indicated that Ni catalyst is structure sensitive toward ammonia decomposition. In their experiment, the turnover rates achieved a maximum value 29.5 s^{-1} while the average Ni particle size is between 1.8 - 2.9 nm. Besides above discussion on catalytic enhancement of Ni based catalysts, other cheap and available catalysts, such as iron and cobalt based catalysts, still are promising candidates for DAFC application due to their low cost. However, those catalysts have a poor catalytic activity compared with Ni and Ru, and few previous researches on high temperature SO-DAFCs utilized those catalyst as

anode materials. Therefore, more studies also should be conducted to enhance the catalytic activity of those catalysts.

4.4 Long-term stability of high temperature SO-DAFCs

Although researches on SOFCs directly fueled with ammonia have attracted massive attention in recent years, few of them includes the specific studies on the long-term stability for high temperature SO-DAFCs. Herein, this section is a short discussion on the stability, also including mechanism of fuel cell performance degradation and possible directions to improve the stability.

As previous work reported, the Ni/YSZ is a state of art anode catalyst for high temperature SO-DAFCs, also the most widely used one due to its high catalytic activity for ammonia decomposition and an ideal peak power density [95-99]. However, researchers found that those SOFCs with Ni/YSZ cermet anode exhibited obvious performance degradation during the long-term operation. A high temperature SO-DAFC experiment conducted by Hagen indicated a 7 % power output degradation at 850 ℃ for over 1500 h stability test, and the Ni/YSZ cermet was used as anode catalyst in his work [118]. Zhang et al. conducted a study on SOFC-O with Ni/YSZ cermet anode catalyst, which observed a 4 % OCV degradation at 800 ℃ for over 100 h stability test [95]. In fact, there are two possible mechanisms that could account for the performance degradation. The first one is that the surface of Ni catalyst could be nitrified by the undecomposed ammonia at low temperature, which would weaken the interaction between Ni and YSZ, resulting in a higher Ohmic resistance during the fuel cell operation. Yang et al. studied the long-term stability of Ni/YSZ anode for high temperature SO-DAFCs. In their experiments, the Ni_3N was identified as a stable phase at 600 ℃, which not only increased the cell resistance but destructed the support layer of anode. Interestingly, the nickel nitrides would be reduced to nickel once temperature elevated above 700 ℃, since the ammonia conversion tended to be more completed, and the formation of nickel nitrides

could be neglected [119]. It should be noted that the operation temperature of the SOFC usually varied within a temperature range, thus SOFC with Ni/YSZ anode operated below or around 600 ℃ would have to consider this kind of degradation. The second degradation mechanism should be nickel particle coarsening during the fuel cell operation. As mentioned in Section 4.3, the Ni based catalyst with a smaller particle size (< 5 nm) usually exhibited a higher catalytic activity. But according to the report of Inokawa et al, those nanoparticle size nickel catalyst tended to be deactivated, resulting from the formation of large particle size at a temperature above 400 ℃ [120]. Recently, an evaluation on high temperature SO-DAFC with Ni/YSZ anode has confirmed this degradation phenomenon in fuel cell operation environment [121]. The stability tests were conducted under 700 ℃ and for 24 hours, indicating a 2 % cell voltage degradation. During the degradation, the enlargements of Ni particles, formation of nickel nitrides accompanied with increase of the ohmic and polarization resistances. Therefore, fueling with ammonia and the high temperature not only deform the microstructure of anode catalyst, but also could be detrimental to electric conductivity.

In order to improve the long-term stability of high temperature SO-DAFCs, there are three possible directions to follow in the future. First of all, combining the ammonia pre-cracking devices with SOFCs could significantly reduce the ammonia centration in the anode chamber, also avoid the formation of nickel nitrides even at a low temperature. Two recent studies on high temperature SO-DAFCs has exhibited a long-term stability for over 1000 hours via developing an external ammonia cracker [122],[123]. Secondly, preparing the Ni based catalysts with bimetallic composition for high temperature SO-DAFC application, since introducing another active metal into Ni based catalyst could inhibit the agglomeration of Ni particles and formation of nickel nitrides. In this case, adding small amount of SrO [123] and Chromium [124] might be a good start to further enhance the stability. The third viable way is

to design other high catalytic activity catalysts for ammonia decomposition, such as Fe and Co based catalysts. In conclusion, the investigation on stability of high temperature SO-DAFCs still in an early stage, which may require further studies in this field.

5. Remaining challenges and future perspectives for DAFCs

For the low temperature AEM-DAFCs, the key challenges are the membrane degradation under alkaline environment, catalyst poisoning issues, and the fuel source ammonia cross-over to the cathode. Those factors could significantly decline the overall fuel cell performance. More importantly, the higher catalytical electro-catalyst for AOR needs to be developed, since the current catalytic activity of anode catalysts within DAFCs still cannot efficiently break the N-H bonds in NH_3 at low temperatures to react with OH^- ions, and suffering from the poisoning effects of the N_{ad} adsorbed on the catalyst surface. While the high temperature SO-DAFCs own a much higher peak power density and better performance than those low temperature DAFCs do, they are still facing issues like incomplete ammonia decomposition and identifying optimal temperature and pressure during the fuel cell operation, also their high operating temperatures are not suitable for electrical vehicles applications.

5.1 Challenges for low temperature AEM-DAFCs

For low temperature AEM-DAFCs, extensive researches have explored on topics regarding identifying suitable electro-catalysts for the anode and cathode of DAFCs and developing alkaline polymeric membranes with high ionic conductivity and low swelling degree. The remaining challenges, however, are to alleviate chemical degradation for membrane, ammonia cross-over and water management during the fuel cell operation, so that a durable membrane and a proper water control method are further required for DAFCs.

Even though AEMs with promising ionic conductivity and mechanical strength have been demonstrated, their chemical stability under alkaline environment still needs further

improvement. Because the chemical instability of cationic functional groups may lead to membrane chemical degradation, as well as the break of polymer backbone or polymer cationic group linkages. In addition, the degradation of cationic groups will decrease the ionic conductivity and increase the ion transport resistance. The QA group was most commonly encountered structure for AEMs within DAFCs. However, the QA group does slowly degrade over time during fuel cell operation. Matthew reported the degradation mechanism of benzyl trim-ethyl ammonium (BTMA), more specifically, the QA group in the BTMA was attacked by hydroxide ions to form various byproducts [125]. As shown in Figure. 8, the primary degradation route (Route 1 and Route 2) is that the substitution reaction on the benzylic carbon or α-carbon, the QA group is attacked, leading to the formation of tertiary amine, benzyl-amine and alcohol byproduct. Also, for a QA group with a β-hydrogen, additional degradation like Hofmann elimination (Route 3) will cause the formation of the tertiary amine, alkenne, and water [126]. Until recently, Dekel proposed that the degradation of QA group could be significantly slowed via operating the fuel cell under a more hydration environment [127]. However, more hydration level will require a good water management ability for DAFCs and hydroxide membrane with a low swelling degree.

On the other hand, water management could be a challenge for the low temperature AEM-DAFCs. Two different models revealed that there is always more water produced at the anode than the cathode, and water production by the ammonia oxidation reaction may cause flooding in the anode. In addition, cathode consumed water molecules, and the dehydration may occur and limit ORR kinetics, especially at high potential region [128],[129]. Besides water issues on the anode and cathode, the hydroxide membrane also requires an adequate hydration level to guarantee the transport of hydroxide ions. Thus, proper water management for DAFCs will be needed to provide enough hydration for membrane without flooding the catalyst or gas diffusion layers [130]. Further, another challenge faced by low temperature

AEM-DAFCs is the cross-over of ammonia. Shohei et al. reported that the formation of N_2 and NO at the cathode was detected for a low temperature AEM-DAFC, so it would be reasonable to induce that the ammonia crossed the membrane was oxidized on the cathode, leading to the reduction in OCV and a lower catalytic activity on the cathode [48].

5.2 Challenges for high temperature SO-DAFCs

Although the high temperature can achieve a much higher power density than ammonia fed fuel cell based on hydroxide membrane, the high operating temperature ($>$ 773 K) limits their application to stationary facilities, also it is hard to identify the optimal temperature and pressure for the fuel cell operation, since the temperature and pressure could significantly influence the overall performance for high temperature SO-DAFC based on various electrode and electrolyte materials. For the effect of operating temperature, a SOFC-O obtained the peak power density of 1190 mW/cm^2 at 650 ℃. However, the peak power density decreased considerably to 167 and 434 mW/cm^2 at 550 ℃ and 600 ℃, respectively. This case could be resulted from the ammonia incomplete decomposition at low temperatures, and these undecomposed ammonia will adsorb on the surface of the anode, which degrades the fuel cell performance [27]. On the other hand, high pressure during the fuel cell operation can cause some problems, related to electrode materials and durability, and also influence the fuel cell performance [131]. Further, the durable performance of high temperature SO-DAFCs suffers from the inferior anode materials and formation of nitrides. In addition, the formation of NO_x will degrade the overall fuel cell performance. The inferior anode materials with undurable anode/electrolyte interface usually cannot sustain the local temperature or pressure change during the fuel cell operation, which will lead to an obvious performance degradation. To completely avoid the formation of NO_x, SOFC-H would be a wise choice. However, SOFC-H has a worse fuel cell performance, since the hydrogen dilution resulted from nitrogen and

unreacted ammonia at anode side [107]. Thus, while the SOFC-H is a preferable choice, its inferior cell performance compared with SOFC-O still needs further improvements.

6. Concluding remarks

To alleviate the carbon emission, ammonia as a low-cost and easy-synthesis chemical is a promising alternative energy source, without problems associated with the traditional hydrogen economy. In recent years, the development of low temperature AEM-DAFCs and high temperature SO-DAFCs have been made to address issues regarding to energy conversion systems. For the low temperature AEM-DAFCs, non-platinum group catalysts were developed with a low cost and higher catalytic activity for the AOR. Also, the hydroxide membrane with a high ionic conductivity and mechanical strength was demonstrated. On the other hand, improvements on the novel electrode and electrolyte materials also have been made for the high temperature SO-DAFCs, as shown in the record, the highest peak power density of 1380 mW/cm^2 at 850 ℃ was obtained. However, the current development for DAFCs is still in an early stage, which is far away from commercialization. As discussed earlier, the low temperature AEM-DAFCs need to address the issues on ammonia cross-over, chemical durability of membrane electrolyte and low catalytic activity electro-catalysts for the AOR. While the high temperature SO-DAFCs need to avoid the incomplete ammonia decomposition and formation of NO_x. Although facing such challenges, DAFCs still perform a promising future in the clean energy field.

Acknowledgements

This work was fully supported by a grant from the Research Grants Council of the Hong Kong Special Administrative Region, China (Project No. 25211817).

References

[1] Züttel, A., Remhof, A., Borgschulte, A., Friedrichs, O. Philos. Trans. R. Soc. A Math. Phys. Eng. Sci. 368 (2010) 3329–3342.

[2] Züttel, A. Mater. Today 6 (2003) 24–33.

[3] Eberle, U., Felderhoff, M., Schüth, F. Angew. Chemie - Int. Ed. 48 (2009) 6608–6630.

[4] Wolf, J. Handbook of fuel cells (2010).

[5] Murray, L. J., Dincă, M., Long, J. R. Chemical Society Reviews 38 (2009) 1294-1314.

[6] Jain, I. P., Jain, P., Jain, A. Journal of Alloys and Compounds 503 (2010) 303-339.

[7] Lim, K. L., Kazemian, H., Yaakob, Z., Daud, W. R. W. Chem. Eng. Technol. 33 (2010) 213–226.

[8] https://www.eurekalert.org/pub_releases/2019-03/w-chs030719.php (accessed on 16 Feb 2020)

[9] Gómez-Gualdrón DA, Colón YJ, Zhang X, Wang TC, Chen YS, Hupp JT. Energy Environ Sci 9 (2016) 3279–89.

[10] Witman M, Ling S, Gladysiak A, Stylianou KC, Smit B, Slater B. J Phys Chem C. 121 (2017) 1171–81.

[11] Goldsmith, J., Wong-Foy, A. G., Cafarella, M. J., Siegel, D. J. Chem. Mater. 25 (2013) 3373–3382.

[12] Rowsell, J. L. C., Yaghi, O. M. Angew. Chemie - Int. Ed. 44 (2005) 4670–4679.

[13] Gómez-Gualdrón DA, Wang TC, García-Holley P, Sawelewa RM, Argueta E., Snurr RQ. ACS Appl Mater Interfaces 9 (2017) 33419–28.

[14] Ahmed A, Seth S, Purewal J, Wong-Foy AG, Veenstra M., Matzger AJ. Nat Commun 10 (2019) 1-9.

[15] Zamfirescu, C., Dincer, I. 185 (2008) 459–465.

[16] https://ammoniaindustry.com/industrial-demonstrations-of-ammonia-fuel-in-japan/ (accessed on 15 Feb 2020)

[17] Erisman, J. W., Sutton, M. A., Galloway, J., Klimont, Z., Winiwarter, W. Nat. Geosci. 1 (2008) 636–639.

[18] https://www.cleantech.com/green-ammonia-potential-as-an-energy-carrier-and-beyond/ (accessed on 12 Feb 2020)

[19] https://www.sciencemag.org/news/2018/07/ammonia-renewable-fuel-made-sun-air-and-water-could-power-globe-without-carbon (accessed on 12 Feb 2020)

[20] Klerke, A., Christensen, C. H., Nørskov, J. K., Vegge, T. J. Mater. Chem 18 (2008) 2304–2310.

[21] Lan, R., Irvine, J. T. S., Tao, S. Int. J. Hydrogen Energy 37 (2012) 1482–1494.

[22] Pan, Z., Bi, Y., An, L. Appl. Energy 258 (2020) 114060.

[23] Pan, Z., Bi, Y., An, L. Appl. Energy 250 (2019) 846–854.

[24] Zhao Y, Setzler BP, Wang J, Nash J, Wang T, Xu B. Joule (2019)1–13.

[25] Afif A, Radenahmad N, Cheok Q, Shams S, Kim JH, Azad AK. Renew Sustain Energy Rev 60 (2016) 822–35.

[26] Lan, R, Tao, S. Frontiers in energy research 2 (2014) 3-6.

[27] Meng, G., Jiang, C., Ma, J., Ma, Q., Liu, X. J. Power Sources 173 (2007) 189–193.

[28] Koo, J., Jang, D. Y., Choi, H. R., Kim, J. W., Shim, J. H. In: Meeting Abstracts. The Electrochemical Society No.48 (2018) pp.1684-1684.

[29] https://www.ammoniaenergy.org/articles/direct-ammonia-fuel-cells-take-another-step-forward-in-japan/ (accessed on 16 Feb 2020)

[30] Cairns, E. J., E. L. Simons., A. D. Tevebaugh. Nature 217 (1968) 780-781.

[31] Hejze, T., Besenhard, J. O., Kordesch, K., Cifrain, M., Aronsson, R. R. J. Power Sources 176 (2008) 490–493.

[32] Yang, J., Muroyama, H., Matsui, T., Eguchi, K., Ag, P. J. Power Sources 245 (2014) 277–282.

[33] Siddiqui, O., Dincer, I. Therm. Sci. Eng. Prog. 5 (2018) 568–578.

[34] Müller, Erich, F. Spitzer. Berichte der deutschen chemischen Gesellschaft 38 (1905) 778-782.

[35] Katan, T., R. J. Galiotto. Journal of The Electrochemical Society 110 (1963) 1022-1023.

[36] Endo, K., Katayama, Y., Miura, T. Electrochimica acta 50 (2005) 2181-2185.

[37] Baltruschat, H. Journal of the American Society for Mass Spectrometry 15 (2004) 1693-1706.

[38] Krausa M., Plats, N. D. La. 39 (1994) 23–31.

[39] Gerischer, H., Mauerer, A. J. Electroanal. Chem. 25 (1970) 421–433.

[40] Liu, Q., Pan, Z., Wang, E., An, L., Sun, G. Energy Storage Mater. (2020).

[41] Katsounaros I, Figueiredo MC, Calle-Vallejo F, Li H, Gewirth AA, Markovic NM. J. Catal. 359 (2018) 82–91.

[42] De Vooys, A. C. A., Koper, M. T. M., Van Santen, R. A., Van Veen, J. A. R. J. Electroanal. Chem. 506 (2001) 127–137.

[43] Jiao, F., Xu, B. Adv. Mater. 1805173 (2018) 1–5.

[44] Endo, K., Katayama, Y., Miura, T. Electrochimica Acta 49 (2004) 1635-1638.

[45] Endo, K., Nakamura, K., Katayama, Y., Miura, T. Electrochimica Acta 49 (2004) 2503–2509.

[46] Lomocso, T. L., Baranova, E. A. Electrochimica Acta 56 (2011) 8551-8558.

[47] Assumpção, M. H., da Silva, S. G., de Souza, R. F., Buzzo, G. S., Spinacé, E. V., Neto, A. O., Silva, J. C. M. Int. J. Hydrogen Energy 39 (2014) 5148–5152.

[48] Suzuki, S., Muroyama, H., Matsui, T., Eguchi, K. J. Power Sources 208 (2012) 257–262.

[49] Assumpção, M. H., Piasentin, R. M., Hammer, P., De Souza, R. F., Buzzo, G. S., Santos, M. C., Silva, J. C. M. Appl. Catal. B Environ. 174 (2015) 136–144.

[50] Katayama, Y., Okanishi, T., Muroyama, H., Matsui, T., Eguchi, K. J. Phys. Chem. C 119 (2015) 9134–9141.

[51] Okanishi, T., Katayama, Y., Muroyama, H., Matsui, T., Eguchi, K. Electrochim. Acta 173 (2015) 364–369.

[52] Silva, J. C. M., da Silva, S. G., De Souza, R. F., Buzzo, G. S., Spinacé, E. V., Neto, A. O., Assumpção, M. H. Appl. Catal. A Gen. 490 (2015) 133–138.

[53] Bonnin, E. P., Biddinger, E. J., Botte, G. G. J. Power Sources 182 (2008) 284–290.

[54] Jiang, J. Electrochem. commun. 75 (2017) 52–55.

[55] Lan, R., Tao, S. Electrochemical and Solid-State Letters 13 (2010) B83-B86.

[56] Little, D. J., Edwards, D. O., Smith, M. R., Hamann, T. W. ACS Appl. Mater. Interfaces 9 (2017) 16488–16494.

[57] Xu, W., Lan, R., Du, D., Humphreys, J., Walker, M., Wu, Z., Tao, S. Appl. Catal. B Environ. 218 (2017) 470–479.

[58] Zhang, H. M., Wang, Y. F., Kwok, Y. H., Wu, Z. C., Xia, D. H., Leung, D. Y. A ChemSusChem 11 (2018) 2889–2897.

[59] Zou, P., Chen, S., Lan, R., Tao, S. ChemSusChem 12 (2019) 2788–2794.

[60] Gottesfeld, S. J. Electrochem. Soc. 165 (2018) J3405–J3412.

[61] Kumar, S., Magotra, V. K., Jeon, H. C., Kang, T. W., Inamdar, A. I., Aqueel, A. T., Ahuja, R. J. Power Sources 402 (2018) 221–228.

[62] Qiao, J., Zhang, J., Zhang, J. J. Power Sources 237 (2013) 1-4.

[63] Lai, A. N., Wang, L. S., Lin, C. X., Zhuo, Y. Z., Zhang, Q. G., Zhu, A. M., Liu, Q. L. ACS Appl. Mater. Interfaces 7 (2015) 8284–8292.

[64] Li, N., Yan, T., Li, Z., Thurn-Albrecht, T., Binder, W. H. Energy Environ. Sci. 5 (2012) 7888–7892.

[65] Benipal, N., Qi, J., Gentile, J. C., Li, W. Renew. Energy 105 (2017) 647–655.

[66] Jasti, A., Shahi, V. K. J. Power Sources 267 (2014) 714-722.

[67] Lee, W. H., Kim, Y. S., Bae, C. ACS Macro Lett. 4 (2015) 814–818.

[68] Fang J, Lyu M, Wang X, Wu Y, Zhao J. J. Power Sources 284 (2015) 517–23.

[69] Pan, Z. F., An, L., Zhao, T. S., Tang, Z. K. Prog. Energy Combust. Sci. 66 (2018) 141–175.

[70] Li, N., Leng, Y., Hickner, M. A., Wang, C. Y. J. Am. Chem. Soc. 135 (2013)10124–10133.

[71] Wang, C., Shen, B., Xu, C., Zhao, X., Li, J. J. Memb. Sci. 492 (2015) 281–288.

[72] Fang, J., Lyu, M., Wang, X., Wu, Y., Zhao, J. J. Power Sources 284 (2015) 517–523.

[73] Yang, Z., Guo, R., Malpass-Evans, R., Carta, M., McKeown, N. B., Guiver, M. D., Xu, T. Angew. Chemie - Int. Ed. 55 (2016) 11499–11502.

[74] Lee, W. H., Kim, Y. S., Bae, C. ACS Macro Lett. 4 (2015) 814–818.

[75] Cremers, C., Niedergesäß, A., Jung, F., Müller, D., Tübke, J. ECS Transactions 41 (2011) 1987-1996.

[76] Zarrin, H., Wu, J., Fowler, M., Chen, Z. J. Memb. Sci. 394–395 (2012) 193–201.

[77] Suzuki, S., Muroyama, H., Matsui, T., Eguchi, K. J. Electrochem. Soc. 163 (2016) F336–F340.

[78] Yan, Y., Xu, B., Wang, J., Zhao, Y. U.S. Patent No. 10,290,890. 14 May 2019.

[79] Hou, H., Wang, S., Jin, W., Jiang, Q., Sun, L., Jiang, L., Sun, G. Int. J. Hydrogen Energy 36 (2011) 5104–5109.

[80] Kim, Y. S., Welch, C. F., Hjelm, R. P., Mack, N. H., Labouriau, A., Orler, E. B. Macromolecules 48 (2015) 2161–2172.

[81] Fujimoto, C., Kim, D. S., Hibbs, M., Wrobleski, D., Kim, Y. S. J. Memb. Sci. 423–424 (2012) 438–449.

[82] Pan, J., Chen, C., Zhuang, L., Lu, J. Acc. Chem. Res. 45 (2012) 473–481.

[83] Ge, Q., Liu, Y., Yang, Z., Wu, B., Hu, M., Liu, X., Xu, T. Chem. Commun. 52 (2016) 10141–10143.

[84] He, S., Liu, L., Wang, X., Zhang, S., Guiver, M. D., Li, N. J. Memb. Sci. 509 (2016) 48–56.

[85] Siddiqui, O., Dincer, I. Fuel Cells 18 (2018) 379–388.

[86] Siddiqui, O. Diss. 300 (2018).

[87] Gottesfeld, S., Dekel, D. R., Page, M., Bae, C., Yan, Y., Zelenay, P., Kim, Y. S. J. Power Sources 375 (2018) 170–184.

[88] Vayenas, C. G., Farr, R. D. Science 208 (1980) 593–594.

[89] Wojcik, A., Middleton, H., Damopoulos, I., Van Herle, J. J. Power Sources 118 (2003) 342–348.

[90] McFarlan, A., Pelletier, L., Maffei, N. J. Electrochem. Soc. 151 (2004) 930–932.

[91] Ni, M., Leung, D. Y. C., Leung, M. K. H. J. Power Sources 183 (2008) 687–692.

[92] Xie, K., Yan, R., Chen, X., Wang, S., Jiang, Y., Liu, X., Meng, G. J. Alloys Compd. 473 (2009) 323–329.

[93] Perman, E. P., G. A. S. Atkinson. Proceedings of the Royal Society of London 74 (1904) 110-117.

[94] Fournier, G. G. M., Cumming, I. W., Hellgardt, K. J. Power Sources 162 (2006) 198–206.

[95] ZHANG, L., You, C. O. N. G., Weishen, Y. A. N. G., Liwu, L. I. N. Chinese Journal of Catalysis 28 (2007) 749-751.

[96] Ma, Q., Ma, J., Zhou, S., Yan, R., Gao, J., Meng, G. J. Power Sources 164 (2007) 86–89.

[97] Molouk, A. F. S., Yang, J., Okanishi, T., Muroyama, H., Matsui, T., Eguchi, K. J. Power Sources 305 (2016) 72–79.

[98] Fuerte, A., Valenzuela, R. X., Escudero, M. J. Daza, L. J. Power Sources 192 (2009) 170–174.

[99] Shy, S. S., Hsieh, S. C. Chang, H. Y. J. Power Sources 396 (2018) 80–87.

[100] Ma, Q., Peng, R. R., Tian, L. Meng, G. Electrochem. commun. 8 (2006) 1791–1795.

[101] Liu, M., Peng, R., Dong, D., Gao, J., Liu, X., Meng, G. J. Power Sources 185 (2008) 188–192.

[102] Maffei, N., Pelletier, L., McFarlan, A. J. Power Sources 175 (2008) 221–225.

[103] Ma, Q., Peng, R., Lin, Y., Gao, J., Meng, G. J. Power Sources 161 (2006) 95–98.

[104] Pelletier, L., McFarlan, A., Maffei, N. J. Power Sources 145 (2005) 262–265.

[105] Xie, K., Ma, Q., Lin, B., Jiang, Y., Gao, J., Liu, X., Meng, G. J. Power Sources 170 (2007) 38–41.

[106] Zhang, L., Yang, W. J. Power Sources 179 (2008) 92–95.

[107] Lin, Y., Ran, R., Guo, Y., Zhou, W., Cai, R., Wang, J., Shao, Z. Int. J. Hydrogen Energy 35 (2010) 2637–2642.

[108] Yang, J., Molouk, A. F. S., Okanishi, T., Muroyama, H., Matsui, T., Eguchi, K. ACS Appl. Mater. Interfaces 7 (2015) 7406–7412.

[109] Chiuta, S., Everson, R. C., Neomagus, H. W., Van der Gryp, P., Bessarabov, D. G. Int J Hydrogen Energy 38 (2013) 14968–91.

[110] Bradford, M. C., Fanning, P. E., Vannice, M. A. Journal of Catalysis, 172 (1997) 479-484.

[111] Chellappa, A. S., Fischer, C. M., Thomson, W. J. Appl Catal A Gen 227 (2002) 231–40.

[112] Schüth, F., Palkovits, R., Schlögl, R., Su, D. S. Energy Environ Sci 5 (2012) 6278–89.

[113] Yin, S. F., Zhang, Q. H., Xu, B. Q., Zhu, W. X., Ng, C. F., Au, C. T. J Catal 224 (2004) 384–96.

[114] Ganley, J. C., Thomas, F. S., Seebauer, E. G., Masel, R. I. Catal Letters 96 (2004) 117–22.

[115] Leybo, D. V., Baiguzhina, A. N., Muratov, D. S., Arkhipov, D. I., Kolesnikov, E. A., Levina, V. V., Kuznetsov, D. V. Int J Hydrogen Energy 41 (2016) 3854–60.

[116] Lucentini, I., Casanovas, A., & Llorca, J. Int J Hydrogen Energy 44 (2019) 12693–707.

[117] Zhang, J., Xu, H., & Li, W. Appl Catal A Gen 296 (2005) 257–67.

[118] Hagen A. Fuel Cells 1608 (2007) 347–56.

[119] Yang, J., Molouk, A. F. S., Okanishi, T., Muroyama, H., Matsui, T., Eguchi, K. ACS Appl Mater Interfaces 7 (2015) 28701–7.

[120] Inokawa, H., Ichikawa, T., Miyaoka, H. Appl Catal A Gen 491 (2015) 184–8.

[121] Stoeckl, B., Subotić, V., Preininger, M., Schwaiger, M., Evic, N., Schroettner, H., Hochenauer, C. Electrochimica acta 298 (2019) 874-883.

[122] Kishimoto, M., Muroyama, H., Suzuki, S., Saito, M., Koide, T., Takahashi, Y.,Takahashi, N. Fuel Cells 20 (2020) 80–8.

[123] Okanishi, T., Okura, K., Srifa, A., Muroyama, H., Matsui, T., Kishimoto, M., Koide, T. Fuel Cells 17 (2017) 383–90.

[124] Hashinokuchi, M., Zhang, M., Doi, T., Inaba, M. Solid State Ionics 319 (2018) 180–5.

[125] Sturgeon, M. R., Macomber, C. S., Engtrakul, C., Long, H., Pivovar, B. S. J. Electrochem. Soc. 162 (2015) F366–F372.

[126] Mohanty, A. D., Bae, C. J. Mater. Chem. A 2 (2014) 17314–17320.

[127] Dekel, D. R., Amar, M., Willdorf, S., Kosa, M., Dhara, S., Diesendruck, C. E. Chem. Mater. 29 (2017) 4425–4431.

[128] Shiau, H. S., Zenyuk, I. V., Weber, A. Z. ECS Transactions 69 (2015) 985-994.

[129] Rasin, I. G., Page, M., Dekel, D. R., Brandon, S. ECS Trans. 80 (2017) 1051–1057.

[130] Omasta, T. J., Peng, X., Lewis, C. A., Varcoe, J. R., Mustain, W. E. ECS Trans. 75 (2016) 949–954.

[131] Kalinci, Y., Dincer, I. Int. J. Hydrogen Energy 43 (2018) 5795–5807.

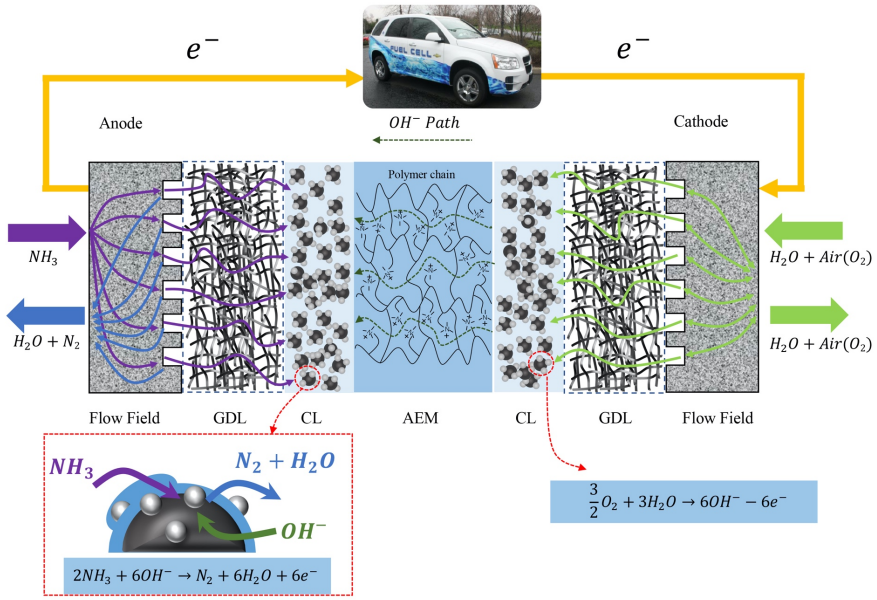

Figure 1 Schematic of a low temperature anion exchange membrane direct ammonia fuel cell.

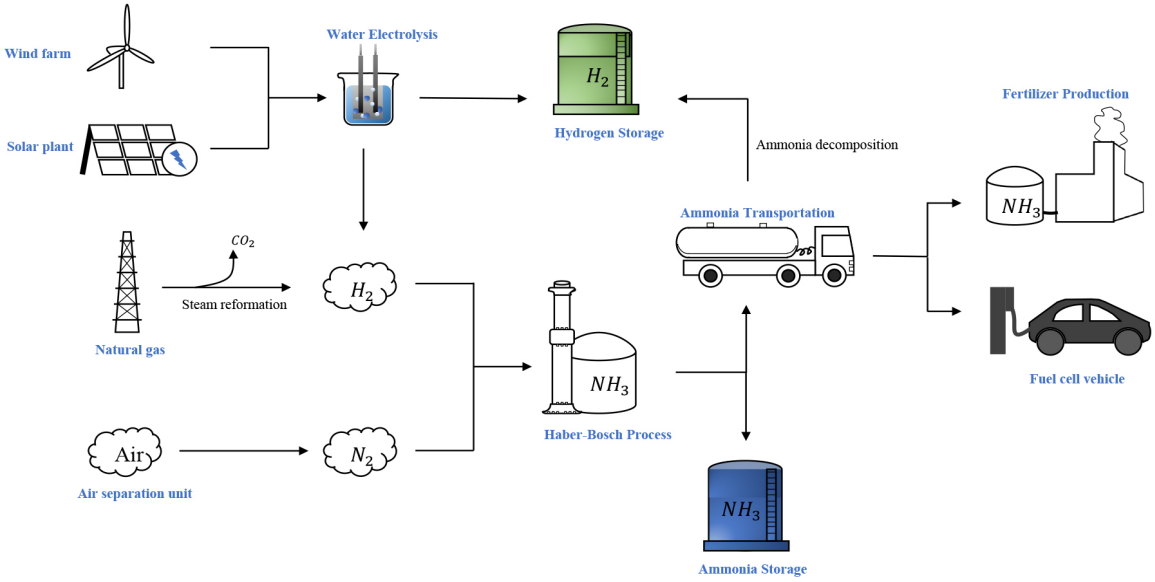

Figure 2 Pathway of ammonia production, distribution and application [21][22]. Reproduced with permission from Elsevier.

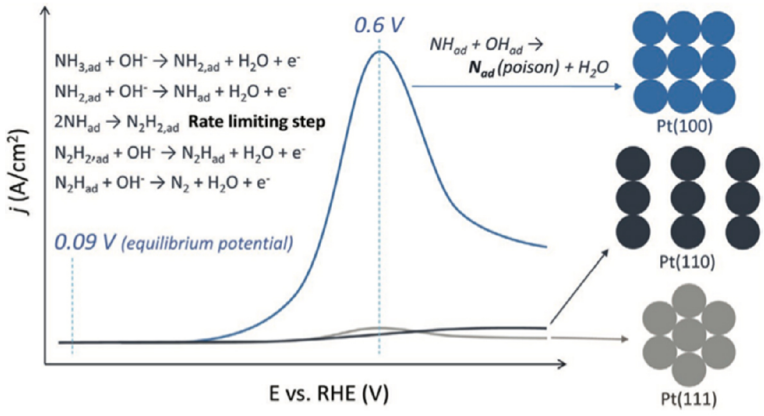

Figure 3 Schematic of the electrochemical ammonia oxidation on different Pt surfaces [38]. Reproduced with permission from Wiley.

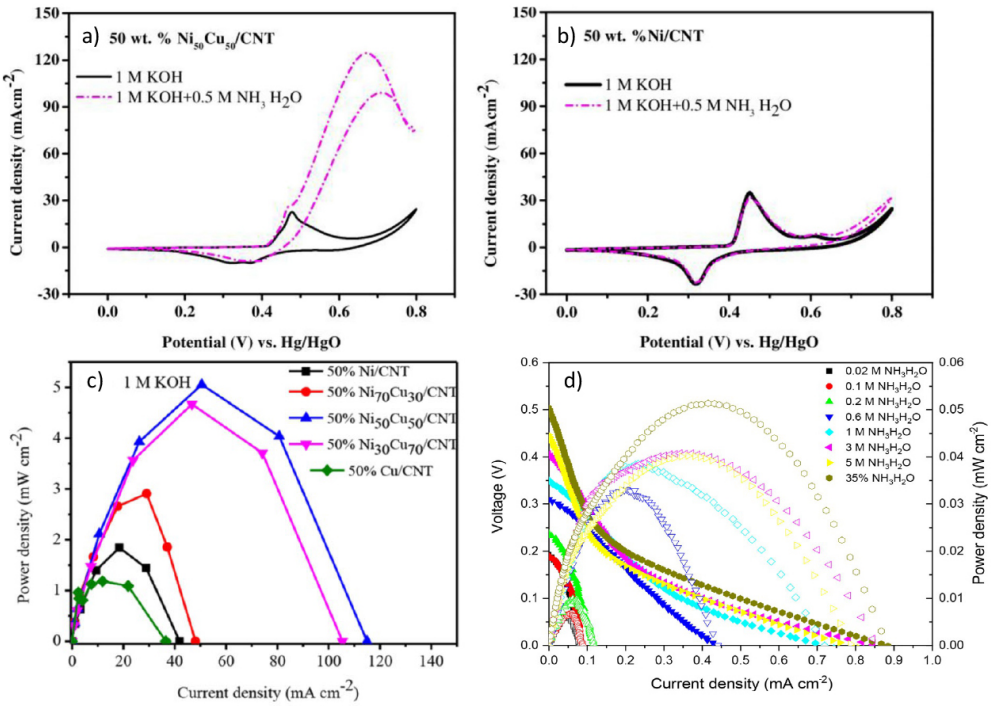

Figure 4 (a) The current density of 50 wt% $Ni_{50}Cu_{50}$/CNTs ; (b) The current density of 50 wt% Ni/CNT; (c) Power density comparison between various catalysts for AOR; [52] Reproduced with permission from Wiley. (d) The peak power density for ammonia fuel cell fabricated with NiCu/C and single phase perovskite oxide [53]. Reproduced with permission from Wiley.

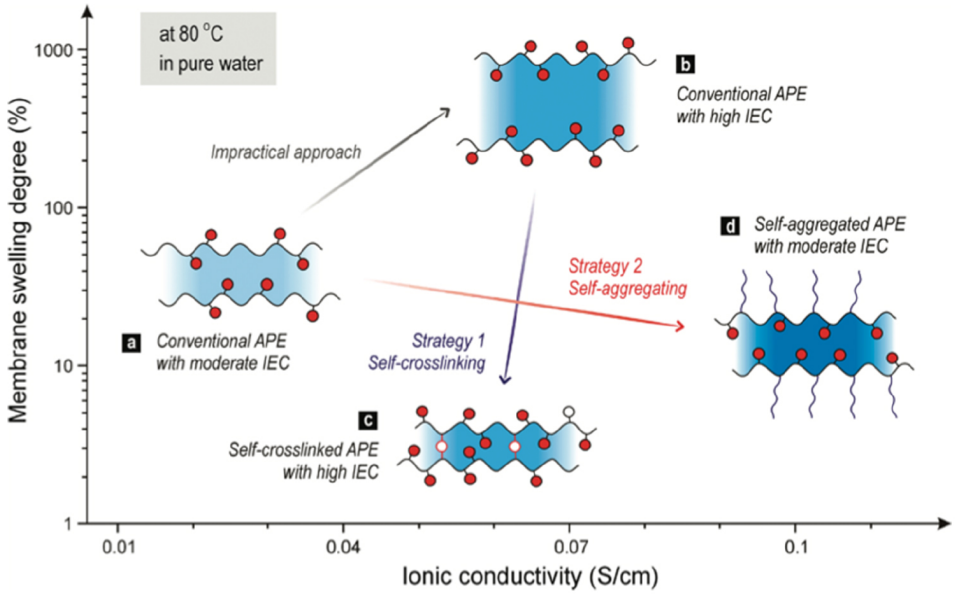

Figure 5 The different strategies for improving mechanical strength of membrane [84]. Reproduced with permission from American Chemical Society.

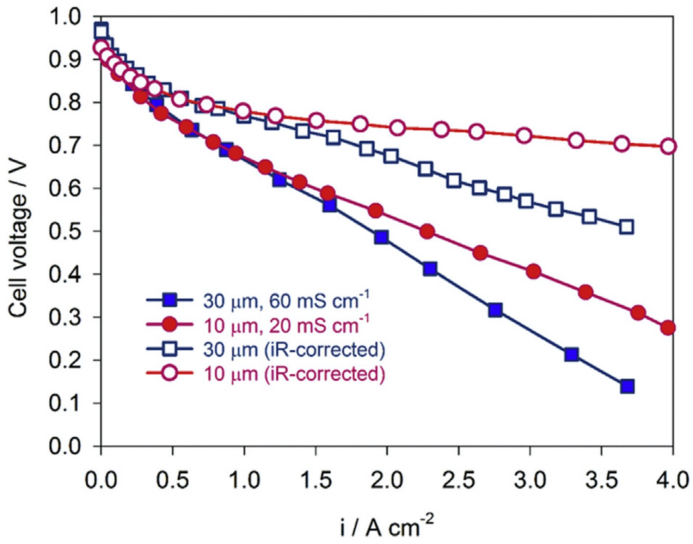

Figure 6 Impact of AEM thickness on H_2/air AEM fuel cell performance operating at 75 °C with fully humidified CO_2-free air at 1 bar (g) (Ag-catalyzed cathode and Pt-catalyzed anode) [72]. Reproduced with permission from Elsevier.

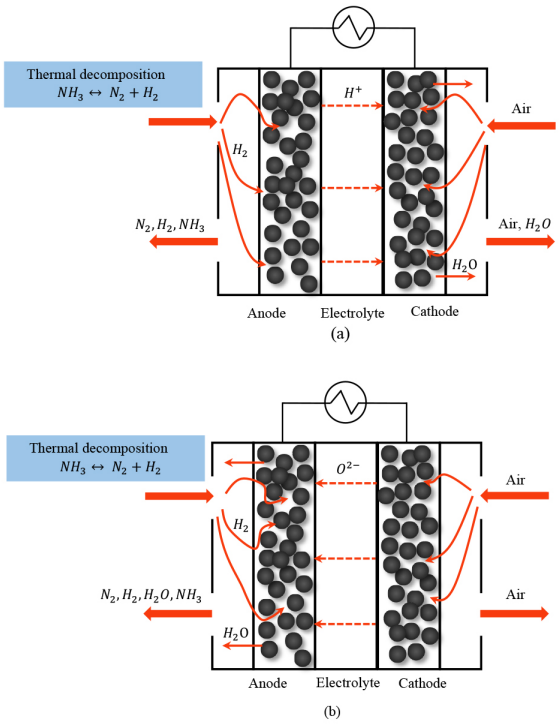

Figure 7 Working principle of high temperature SO-DAFCs (a) proton conducting type (SOFC-H) (b) anion conducting type (SOFC-O). [25] Reproduced with permission from Elsevier.

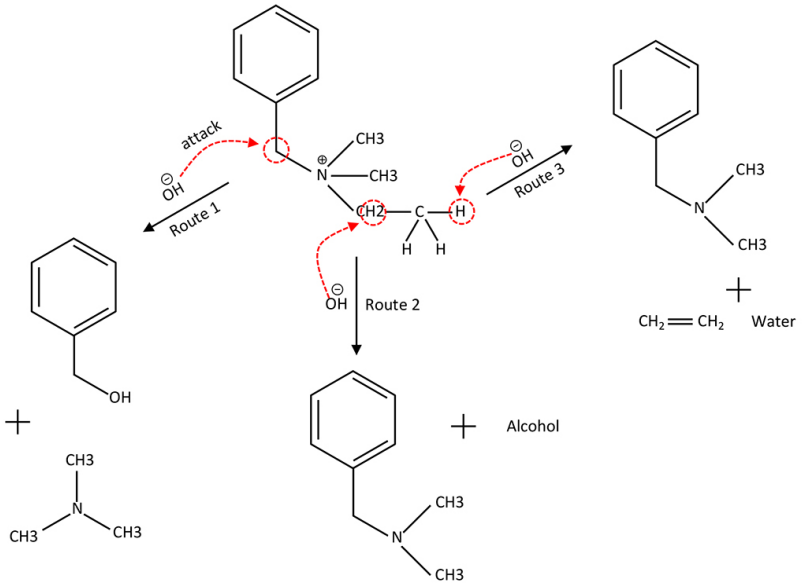

Figure 8 Schematic of the QA groups degradation routes. [126]

Anode	Cathode	Membrane electrolyte	Fuel	Temperature(°C)	OCV (V)	Peak power density (mW/cm^2)	Reference
Pt/C with Pt loading 0.5 $mg\ cm^{-2}$	Pt/C with Pt loading 0.5 $mg\ cm^{-2}$	AEM (A201, Tokuyama Corp.)	NH_3	50	0.37	~4.76	[31]
Pt-Ru/C with Pt loading 0.5 $mg\ cm^{-2}$	Pt/C with Pt loading 0.5 $mg\ cm^{-2}$	AEM (A201, Tokuyama Corp.)	NH_3	50	0.54	~3.07	[31]

Pt-Rh/C with metal loading 2.0 $mg\ cm^{-2}$	Pt/C with Pt loading 2.0 $mg\ cm^{-2}$	Modified Nafion 117	3 M NH_4OH -3 M KOH	50	0.68	5.37	[43]
SnO_2-Pt/C with Pt loading 0.4 $mg\ cm^{-2}$	Pt/C with Pt loading 0.4 $mg\ cm^{-2}$	AEM (A201, Tokuyama Corp.)	NH_3	50	~0.40	~4.15	[45]
Pt-Ir/C	Pt/C	Modified Nafion 117	5 M NH_4OH -1 M KOH	40	0.716	4.17	[42]
Ir/C	Pt/C	Modified Nafion 117	3 M NH_4OH -1 M KOH	40	0.408	1.32	[42]
Pt-Au/C with Pt loading 1.0 $mg\ cm^{-2}$	Pt/C with Pt loading 1.0 $mg\ cm^{-2}$	Modified Nafion 117	5 M NH_4OH -1 M KOH	40	0.588	2.64	[46]
Au/C with Au loading 1.0 $mg\ cm^{-2}$	Pt/C with Pt loading 1.0 $mg\ cm^{-2}$	Modified Nafion 117	1 M NH_4OH -1 M KOH	40	0.289	0.516	[46]
Cr-decorated Ni/C with loading 10 $mg\ cm^{-2}$	MnO_2/C with loading 20 $mg\ cm^{-2}$	AEM (CPPO-PVA)	35% NH_3	25	0.85	16	[30]
$Ni_{50}Cu_{50}$/CNTs	Pt/C with Pt loading 2.0 $mg\ cm^{-2}$		1 M NH_3-3 M KOH	25	1.31	10.94	[52]
NiCu/C with loading 2.5 $mg\ cm^{-2}$	$SrCo_{0.8}Cu_{0.1}Nb_{0.1}O_{3-\delta}$ with loading 18.67 $mg\ cm^{-2}$	FAA AEM	35% NH_3- 1 M NaOH	25		0.25	[53]
Pt/C with Pt loading 2.0 $mg\ cm^{-2}$	PGM-free	AEM (unspecified)	NH_3	100		420	[54]
Pt-Ir/C with Pt loading 2.0 $mg\ cm^{-2}$	Acta 4020 with loading 1.0 $mg\ cm^{-2}$	AEM (PAP-TP)	3 M NH_3-1 M KOH	80	0.63	121	[24]
Pt-Ir/C with Pt loading 2.0 $mg\ cm^{-2}$	Acta 4020 with loading 1.0 $mg\ cm^{-2}$	AEM (PAP-TP)	3 M NH_3-3 M KOH	80	0.63	135	[24]

Table 1. The summary of low temperature direct ammonia fuel cell performances with various electro-catalysts.

	Anode	Cathode	Electrolyte	Operating temperature (℃)	OCV (V)	Peal
SOFC-O	NiO-YSZ	LSM-YSZ	YSZ	650	1.08	
	NiO-YSZ	LSM-YSZ	YSZ	750	1.07	
	NiO-YSZ	LSM-YSZ	YSZ	850	1.03	
	Ni-YSZ	YSZ-LSM	YSZ	800	1.06	
	Ni-YSZ	LSM	YSZ	700	1.03	
	Ni-YSZ	LSM	YSZ	800	1.02	
	Ni-YSZ	LSM	YSZ	900	0.99	
	Ni-YSZ	LSC-GDC	YSZ	750		
	Ni-YSZ	LSC-GDC	YSZ	800		
	Ni-YSZ	LSC-GDC	YSZ	850		
	Pt-YSZ	Ag	YSZ	800	0.9	
	Pt-YSZ	Ag	YSZ	900	0.9	
	Pt-YSZ	Ag	YSZ	1000	0.9	
	Ni-SDC	SSC-SDC	SDC	500	0.9	
	Ni-SDC	SSC-SDC	SDC	600	0.88	
	Ni-SDC	SSC-SDC	SDC	700	0.83	
	NiO-SDC	SSC-SDC	SDC	650	0.79	
	NiO	BSCF	SDC	550	0.795	
	NiO	BSCF	SDC	600	0.771	
	NiO	BSCF	SDC	650	0.768	
SOFC-H	NiO-BCE	Pt	BCGP	500		
	NiO-BCE	Pt	BCGP	550		
	NiO-BCE	Pt	BCGP	600	0.92	
	NiO-BCGO	LSCO-BCGO	BCGO	600	1.102	
	NiO-BCGO	LSCO-BCGO	BCGO	650	1.095	
	NiO-BCGO	LSCO-BCGO	BCGO	700	0.985	
	NiO-BCGO	LSCO-BCGO	BCGO	750	0.963	
	Pt	Pt	BCGP	700	0.85	
	Pt	Pt	BCG	700	0.85	
	NiO-BCNO	LSCO	BCNO	700	0.95	

	Ni-CGO	BSCFO-CGO	BCGO	600	1.12
	Ni-CGO	BSCFO-CGO	BCGO	650	1.10
	NiO-BZCY	BZCY	BSCF	450	
	NiO-BZCY	BZCY	BSCF	500	
	NiO-BZCY	BZCY	BSCF	550	
	NiO-BZCY	BZCY	BSCF	600	
	NiO-BZCY	BZCY	BSCF	650	
	NiO-BZCY	BZCY	BSCF	700	
	NiO-BZCY	BZCY	BSCF	750	
	Ni/BCY25/SSC	Pt	BCY10	600	1.07
	Ni/BCY25/SSC	Pt	BCY10	650	1.05

Table 2. The summary of high temperature direct ammonia fuel cell performances for various electrode and electrolyte materials [35]. Reproduced with permission from Elsevier.

	Advantages	Challenges	Future Research Directions
Low temperature AEM-DAFCs	•A low operating temperature (25 - 100 ℃), which could be a candidate for electric vehicle application •A promising peak power density (420 mW/cm^2) could be achieved with non-platinum-group metal catalysts	•The peak power density still lower than fuel cells with hydrogen, and catalyst poisoning issues for AOR •Degradation of membrane electrolytes •Ammonia crossover	•Novel non-platinum-group metal catalyst design with a high catalytic activity for AOR and no formation of surface poisons on the catalyst. •Figuring out the effects of operating temperature and hydroxide concentration on AOR activity of distinct platinum-free catalysts •The thinner membrane electrolyte with good chemical stability and low ammonia permeation should be designed
High temperature SO-DAFCs	•A much higher peak power density than low temperature AEM-DAFCs	•Incomplete ammonia decomposition at low operating temperatures •Issues on catalyst deactivation and fuel cell long-term operation stability	•Further enhancement on catalytic activity of catalysts at low temperatures, which could start from design of bimetallic catalysts, particle-size control of Ni-based catalysts and the development of Fe- and Co-based catalysts •Adding the ammonia pretreatment to high temperature SO-DAFC system, or designing Ni-based catalysts with bimetallic composition to avoid formation of nickel nitrides and enlargement of Ni particle size

Table 3. The summary for two types of direct ammonia fuel cell